Russian Chemical Reviews **82** (10) 917–941 (2013) © 2013 Russian Academy of Sciences and Turpion Ltd

DOI 10.1070/RC2013v082n10ABEH004366

Chemical modification of nanocrystalline tin dioxide for selective gas sensors

V V Krivetskiy, M N Rumyantseva, A M Gaskov

Contents

I. Introduction 917
II. Chemical interaction of metal oxide surfaces with gases 920
III. Effect of modifiers on the sensing properties of nanocrystalline tin dioxide 924
IV. Conclusion 939

Abstract. Chemical methods for enhancement of the selectivity of semiconductor metal oxide gas sensors are considered taking SnO_2 as an example. Theoretical concepts concerning correlations between the metal oxide chemical composition, crystal structure, surface morphology and the oxide surface reactivity are discussed. Application of such concepts to the design of novel, highly selective sensor materials based on nanocrystalline SnO_2 is discussed in detail. Experimental data on the determination of the chemical composition, structure, activity in gas–solid chemical interaction and the sensor properties of such materials are analyzed. The applicability of modern concepts of the chemical activity of the surface in gas–solid reactions to the design of novel metal oxide sensor materials with enhanced selectivity is substantiated. The bibliography includes 133 references.

I. Introduction

Chemical gas sensors are widely used to obtain information on the environment, in scientific research and in industry for analysis of the composition of various process gas phases, for control of physiological state of human subjects, food quality, *etc*.[1–3] In this connection, intensive research on the design of novel materials with high sensitivity towards particular types of gases is carried out. Semiconductor oxides SnO_2, ZnO, WO_3 and In_2O_3 are of paramount interest for the design of gas sensors.[4] In these cases, the sensor signal is produced by reversible changes in the concentration of charge carriers in the near-surface layer as a result of chemical reactions on the surface. Conductivity changes (analytical signal) can also be due to direct transfer of electron density between adsorbed gas molecules and the solid surface.[5–7] The conductivity of wide-gap semiconductors is highly sensitive to the state of the surface at 300–800 K. In this temperature range, redox reactions occur on the surface of oxides. The surface of oxides is characterized by high adsorption properties and high reactivity due to the presence of (i) free electrons in the conduction band, (ii) oxygen vacancies on the surface and in the bulk material, and (iii) reactive chemisorbed oxygen.[8,9] The most widely used material for semiconductor gas sensors is tin dioxide SnO_2 with n-type conductivity, high adsorption capacity, high chemical and thermal stability in air; the band gap of SnO_2 is 3.6 eV (300 K).

The key properties of sensor materials include reversibility of their state upon cyclic changes in the chemical composition of the environment. Taking into account this fact, chemical interaction between the surface of a semiconductor oxide and the gas phase can be schematically represented as a cyclic process (Fig. 1). The complex interaction mechanism involves physisorption and chemisorption of molecules on the oxide surface. If atmospheric air contains no impurities, the main components of adsorption layer include water molecules, hydroxyl groups and chemisorbed oxygen, which can exist in the form of molecular (O_2^-) and atomic (O^-, O^{2-}) ions depending on particular conditions.[10] Chemisorption of molecular oxygen from atmospheric air is accompanied by localization of conduction-band electrons on the molecules and subsequent bending of energy bands in a thin layer near the surface of semiconductor grains. The conductivity of the material depends on the concentration and type of species chemisorbed on the oxide surface. In the presence of impurities in air, chemisorbed oxygen can react with the impurities. Such chemical reactions involve electron exchange between the surface and the bulk of the semiconductor and cause an increase or a decrease in the conductivity, which is measured and treated as the sensor signal. Gaseous products of the gas–solid interaction are desorbed from the surface while the chemisorbed forms of oxygen consumed during

V V Krivetskiy, M N Rumyantseva, A M Gaskov Department of Chemistry, M V Lomonosov Moscow State University, Leninskie Gory 1, 119991 Moscow, Russian Federation. Tel. (7-495) 939 54 71, e-mail: vkrivetsky@inorg.chem.msu.ru (V V Krivetskiy), roum@inorg.chem.msu.ru (M N Rumyantseva), gaskov@inorg.chem.msu.ru (A M Gaskov)

Received 26 December 2012
Uspekhi Khimii **82** (10) 917–941 (2013); translated by A M Raevskiy

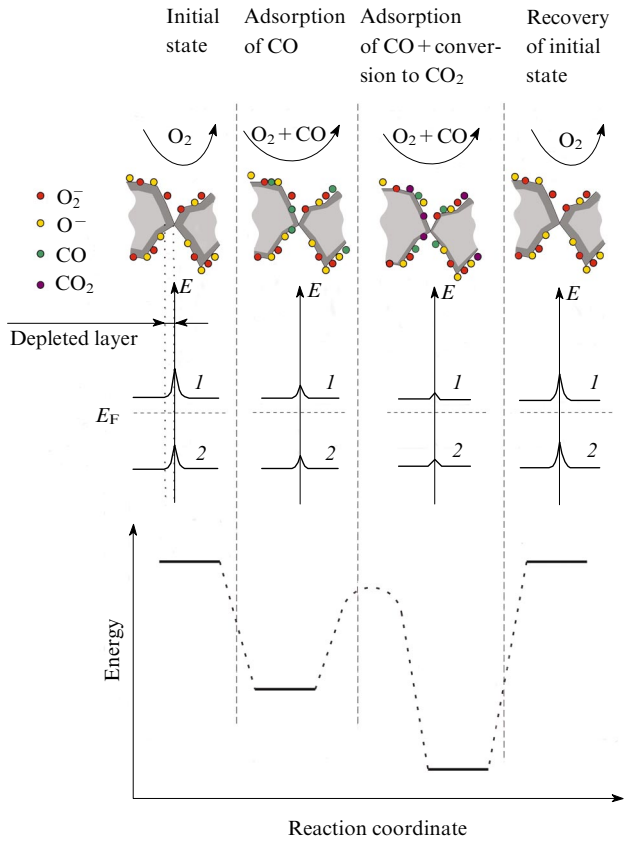


Figure 1. Interaction of CO with the surface of nanocrystalline SnO_2 accompanied by changes in degree of bending of the conduction band (*1*) and valence band (*2*) of the semiconductor, in the semiconductor conductivity and by the formation of sensor response.

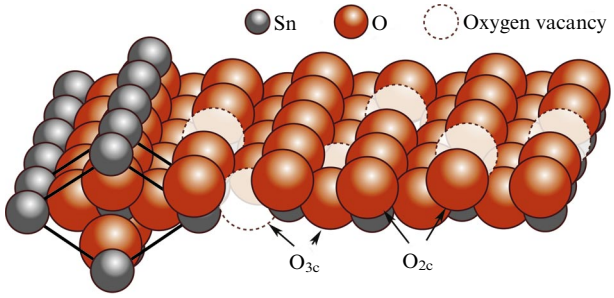


Figure 2. $SnO_2(110)$ surface: a schematic.
The marked oxygen vacancies are sites for non-specific adsorption of gas molecules.

the interaction are compensated in the course of dissociative adsorption of oxygen on the surface. As a result, the conductivity of the sensor material is recovered provided that the atmosphere is free from impurities.

This cycle shows a great similarity between sensor materials and catalysts of heterogeneous reactions; active centres of such reactions are also involved in a catalytic cycle. The main difference between the sensor materials and catalysts consists in that the interaction of the former with components of the gas phase should first of all ensure maximum changes in the intrinsic fundamental properties (electrical, optical and magnetic ones) rather than the yield of reaction products.

Low selectivity is critical to the sensor materials based on semiconductor oxides. In this case, it is impossible to select the contribution of a particular type of molecules to the overall changes in the conductivity. Low selectivity of sensor materials based on nanocrystalline SnO_2 is due to the fact that the surface of the semiconductor grains is covered with various active centres including a large proportion of oxygen vacancies (Fig. 2). Active centres make the SnO_2 surface able to simultaneously interact with different gas molecules.

Low selectivity is particularly pronounced in the case of highly reactive gas molecules. The problem of selectivity becomes of great importance when the range of air pollutants is extended and when the maximum permissible concentrations of the pollutants declared in the health and safety regulations differ appreciably, *viz.*, ranging from a few mass percent to a few thousandth of a mass percent. In this connection, the need to enhance the specificity of the chemical properties of the surface of semiconductor oxides in reactions with gaseous impurities in air against the background of poisoning or masking components comes to the fore.

Specialists from various research groups demonstrated a variety of physical and chemical approaches to the problem of selectivity enhancement of gas-sensitive materials, *e.g.*, utilization of semi-permeable [11] or catalytic [12] membranes on the surface of sensitive layers as well as dynamic temperature regimes of sensor operation.[13] However, the most promising and versatile is the method of chemical modification of the sensor material, *i.e.*, targeted variation of the surface state, creation of active sites for specific chemical interaction with the gas to be detected, accompanied by a decrease in the concentration of the centres of non-selective interaction. Chemical modification leads to a more pronounced differentiation of functions between the surface ('receptor') and bulk ('converter') in a complicated process of formation of the sensor signal. The efficiency of such an approach to enhancement of the selectivity and sensitivity of sensor materials has been demonstrated (see, *e.g.*, Refs 14–21).

The role of modifiers can be played by Au, PdO_x, PtO_x and RuO_x clusters as well as d-element oxides (CuO, NiO, Fe_2O_3, MoO_3, V_2O_5, *etc.*) distributed over the surface of nanocrystalline SnO_2 grains. Experimental investigations of such materials by X-ray diffraction methods including synchrotron radiation, by scanning and transmission electron microscopy, by X-ray spectroscopic methods [in particular, energy-dispersive X-ray spectroscopy (EDX)] and other techniques revealed their complex structure (Fig. 3). Clusters consisting of modifier species change the state of the surface and can also be constituent parts of grains and replace tin atoms in the cation sublattice, thus forming solid solutions with SnO_2.[21–29] The bulk-to-surface modifier concentration ratio depends strongly on the degree of dispersion of SnO_2 and on the synthesis temperature.[21] Distribution of modifiers across the surface and over the bulk of the semiconductor grain is accompanied by the

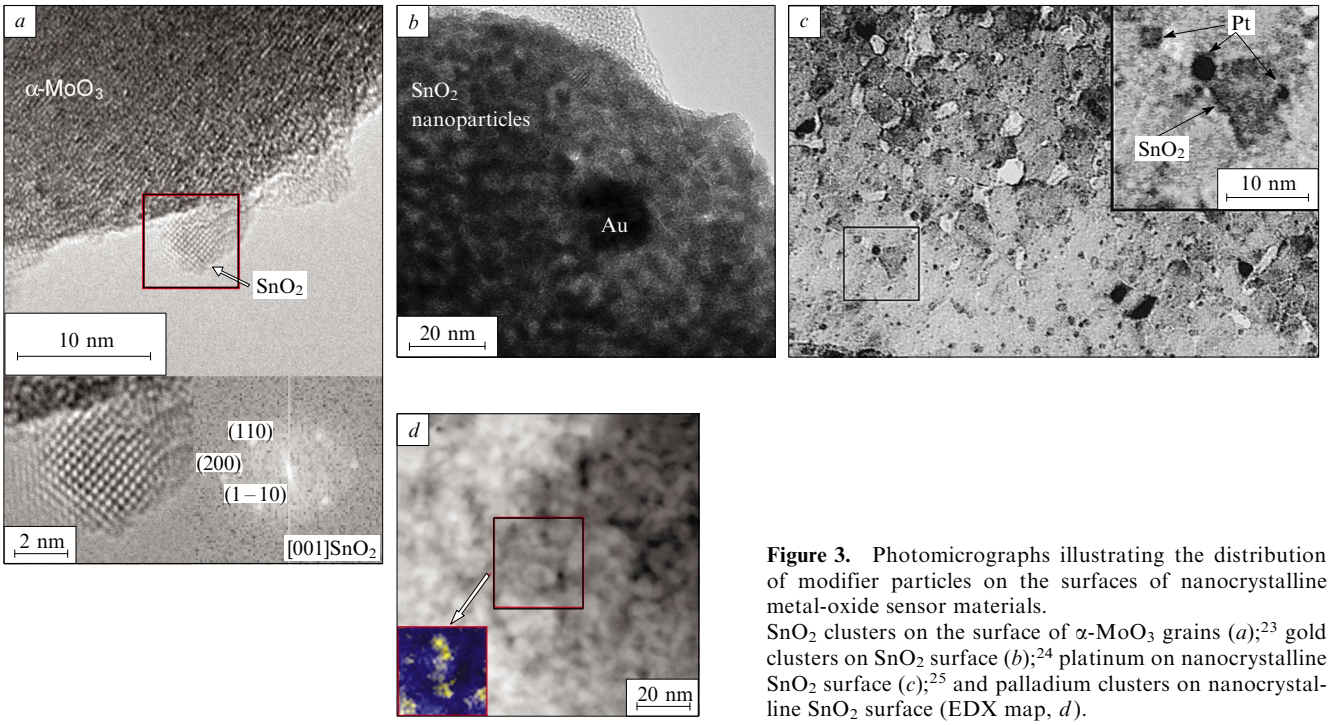


Figure 3. Photomicrographs illustrating the distribution of modifier particles on the surfaces of nanocrystalline metal-oxide sensor materials.
SnO_2 clusters on the surface of α-MoO_3 grains (*a*);[23] gold clusters on SnO_2 surface (*b*);[24] platinum on nanocrystalline SnO_2 surface (*c*);[25] and palladium clusters on nanocrystalline SnO_2 surface (EDX map, *d*).

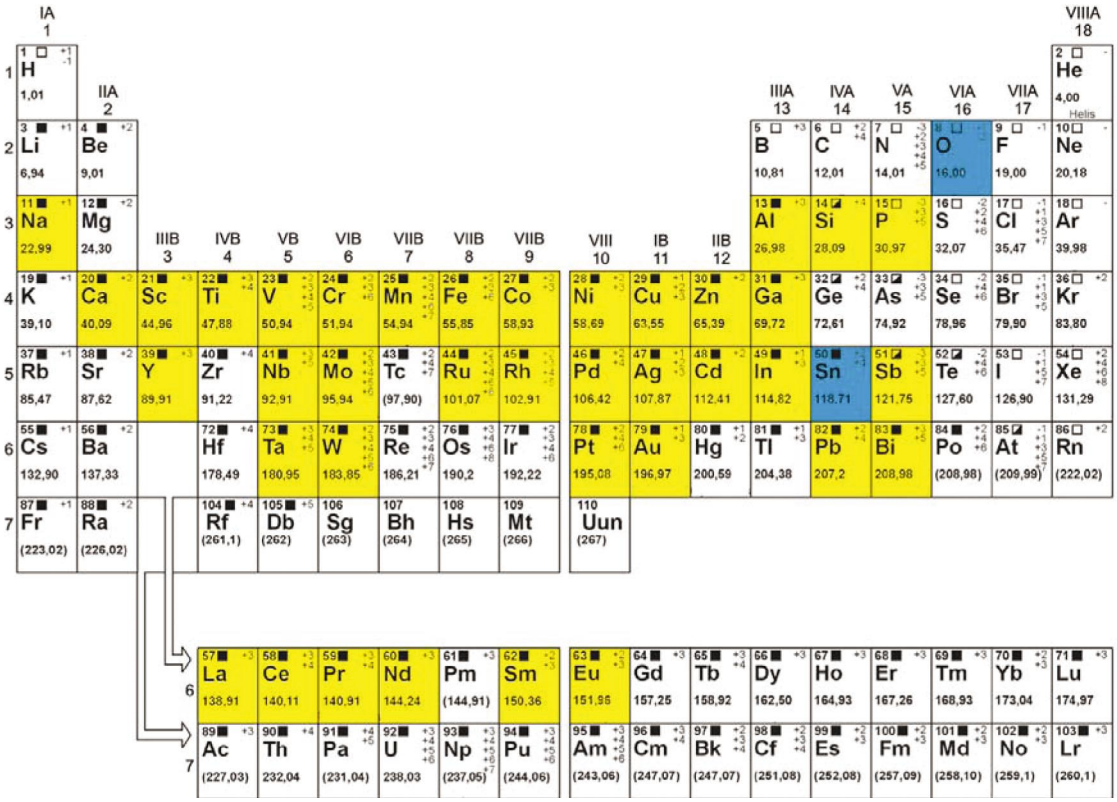


Figure 4. Chemical elements (shown in yellow) tested as modifiers of nanocrystalline SnO_2 in the design of novel materials for gas sensors.

formation of new adsorption sites.[21] This imparts new chemical properties to the sensor material, which enable specific interaction between the material and gas molecules.

However, a formal theory of targeted choice of paticular modifiers has not been developed so far.[30] This is to some extent due to predominance of research (and, correspondingly, publications) on sensor materials including oxide semiconductors, from the standpoint of solid state physics, namely, the energy band theory and percolation mechanism of conduction.[10, 31]

At the same time, electron density transfer between the semiconductor and the component to be detected is, on the one hand, a necessary condition for the emergence of a sensor response and, on the other hand, a kind of chemical interaction because it involves adsorption and chemical transformations on the surface which often occur involving some extra chemisorbed species. Therefore, a targeted choice of a modifier can be based on fundamental ideas of its reactivity towards different types of gases. Nevertheless, studies on reasoned choice of modifiers for the sensor materials are scarce. The design of gas sensors based on SnO_2 was accompanied by tests of noble metals and s-, p-, d- and f-element oxides (Fig. 4) for being modifiers. Most results were obtained by the 'trial and error' method and no correlations between the chemical properties of the modifier and the gas to be detected were established.

In spite of a large body of available experimental data on the design of semiconductor sensor materials, it is impossible to make inferences suitable for unambiguous prediction of the nature of the modifier with optimum properties for successful selective detection of a particular gas. At the same time, researchers working in the field of heterogeneous catalysis not only did accumulate a huge body of experimental data, but also proposed a number of concepts concerning the regularities of chemical interaction between the solid surfaces and gas molecules.[32–35] The difference between the catalyst of a heterogeneous chemical process and the sensor material shoud be emphasized again. Emergence of a pronounced sensor response as a result of a catalytic reaction on the surface of some material requires that the reaction be accompanied by changes in the electron density in the conduction band of the semiconductor. These changes can be due to direct electron transfer from the adsorbed molecules to the bulk of the solid in the course of reaction and to bending of the energy bands due to adsorption on the surface.[36]

Taking into account the similarity and differences between catalytic and sensor materials (see above), in this review we will discuss the applicability of these formal approaches to targeted modification of nanocrystalline SnO_2 in order to design sensor materials with selective response towards various gases.

II. Chemical interaction of metal oxide surfaces with gases

1. Adsorption of gases on metal oxide surfaces

The interaction of a gas molecule with a solid surface can be described by a number of consecutive steps including adsorption, chemical reaction and desorption of reaction products:

$$A_0 + R_{(gas)} \xrightarrow{\text{adsorption}} R_{(ads)}/A_1 \quad (1)$$

$$R_{(ads)}/A_1 \xrightarrow{\text{reaction}} R'_{(ads)}/A_2 \quad (2)$$

$$R'_{(ads)}/A_2 \xrightarrow{\text{desorption}} A_3 + R'_{(gas)} \quad (3)$$

$$A_3 + R'_{(gas)} \xrightarrow{\text{recovery}} A_0 \quad (4)$$

where A_0 is the solid surface in the initial state, $R_{(gas)}$ is the initial gas molecule in the gas phase, $R_{(ads)}$ is the gas molecule adsorbed on the solid surface, A_1 is the solid surface after chemisorption of the gas molecule, $R'_{(ads)}$ is the adsorbed product of the chemical interaction between the gas molecule and the solid surface, A_2 is the solid surface after chemical reaction involving the adsorbed molecule, $R'_{(gas)}$ is the gaseous product of the chemical interaction and A_3 is the solid surface after desorption of reaction products. For both catalytic materials and sensor materials, the cycle is completed with recovery of the oxide surface to the initial state A_0.

Adsorption is the first step in the gas–solid interaction. Adsorption (chemisorption) of gas molecules on metal oxide surfaces is usually studied from the standpoint of the Lewis theory of acid-base interaction.[37] The role of active adsorption sites on metal oxide surfaces is played by coordinatively unsaturated metal atoms. Electron-deficient cations exhibit the properties of Lewis acids towards most electron-rich gas molecules. The excess electron density is formed by electron pairs and unpaired electrons occupying higher molecular orbitals. For this reason, adsorption of gases on the SnO_2 surface occurs as a result of their acid-base interaction with metal cations, accompanied by partial transfer of electron density. In turn, oxygen anions become adsorption sites only for strong Lewis acids, *i.e.*, metal cations, organic molecules having the properties of Brønsted acids, cations produced upon heterolytic dissociation of species adsorbed on the oxide surface or those that underwent heterolytic dissociation in the gas phase.

Thus, an increase or a decrease in the strength/concentration of the acid and basic adsorption sites on modified SnO_2 surfaces can be utilized to enhance or reduce the activity of the sorption interaction of the sensor material with particular gas molecules. This type of surface modification is used to design catalysts[38, 39] or chemical gas sensors.[40, 41]

The acidity of the modified materials can be determined by modern methods of investigation of the acid properties of the surface of materials, *e.g.*, IR spectroscopy of probe molecules,[42, 43] temperature-programmed desorption[44] and microcalorimetric methods.[45] However, prediction of acidity increase or decrease for the surface of oxide materials as a result of modification of the oxide component is still impossible. It is to be emphasize that the acidity of individual metal cation on the oxide surface is governed by a number of parameters including the type and oxidation state of the atom, the number of vacancies in the anionic environment and some other factors that are different for the oxidized and reduced surfaces.[37] The reactivity (in particular, acidity) of the metal oxide surface is closely related to the bulk properties of phases.[32] Because of this, we believe that classification of simple oxides of various metals with respect to acidity of their surfaces using quantitative data on the properties of bulk oxide phases may

appear to be the starting point in the design of novel sensor materials.

The available methods of evaluating the Lewis acidity of oxide surfaces utilize the electronegativity, a fundamental chemical property of atoms that form the oxide compound. In addition, a number of bulk properties such as the partial atomic charges of the metal (q_M) and oxygen (q_O) components of oxides, correlations between the metal–oxygen bond strength and reactivities of oxide materials, the Madelung potential, cation polarizabilities, *etc.* are also discussed.[32]

2. The optical basicity

A modern approach to classification of various metal oxides with respect to their Lewis acidity[46] is based on the concept of so-called optical basicity (Λ)[47] and on the Zhang electronegativities of cations.[48,49] The optical basicity is a measure of the bathochromic shift of the characteristic UV absorption bands of an oxide. The characteristic bands correspond to $^1S_0 \rightarrow {}^3P_1$ transition of the probe ions (Tl^+, Pb^{2+} or Bi^{3+}) incorporated into the oxide matrix in order to measure the acidity in the bulk of the oxide material. The bathochromic shift is due to extension of outer electron orbitals of the probe cations owing to the shielding action of the electron density of the surrounding oxygen anions, which in essence is acid-base interaction. This is the nephelauxetic effect, which is best described for complex compounds of d-elements.[50,51] By measuring the shift of the energy levels of the probe cations incorporated into the oxide matrix one can evaluate the strength of corresponding acid-base interaction. According to Duffy,[47] the Lewis acidity of the oxide-forming cations is inversely proportional to their optical basicity. The optical basicity of complex oxide systems (Λ_{th}) is an additive quantity:[52]

$$\Lambda_{th} = X_{AO_{a/2}} \Lambda_{AO_{a/2}} + X_{BO_{b/2}} \Lambda_{BO_{b/2}} + \ldots \quad (5)$$

where $\Lambda_{AO_{a/2}}$, $\Lambda_{BO_{b/2}}$ ... are the optical basicities of the oxides $AO_{a/2}$, $BO_{b/2}$ ...; and $X_{AO_{a/2}}$, $X_{BO_{b/2}}$ ... are the proportions of oxygen atoms from all individual oxides present in the system. Using the additivity principle, one can calculate the bulk property which characterizes the acidity of cations in the bulk of a complex oxide compound provided that the optical basicity values of simple oxides are known.

Direct measurements of the optical basicities of oxides by spectroscopic methods are impossible because of strong absorption of UV radiation. Therefore, for most cations that are present in different electronic states and coordination environments,[53,54] the optical basicity values were determined from computations.[46] Calculations were carried out using the so-called ionic-covalent parameter (ICP) that simultaneously characterizes the ionic and covalent contributions to the formation of the metal–oxygen bond in the oxide compound[55]

$$\mathrm{ICP} = \log\left(\frac{Z}{r_i^2}\right) - A\chi_i + B \quad (6)$$

where Z is the formal charge of the cation, r_i is the ionic radius and χ_i is the Zhang electronegativity;[48,49] the coefficients A and B are chosen in such a manner that the ICP of Au^+ cation is zero.[56]

The Au^+ cation was chosen as a reference because of very low acidity and instability of its compounds with even very strong bases.

Correlations between the Lewis acidity and fundamental properties of compounds can be used to predict the reactivities of not only individual oxides, but also composite materials based on them. The applicability of this approach to evaluation of the Lewis acidity of oxide materials was demonstrated in studies on heterogeneous catalysis.[46,57]

Other correlations between the optical basicity and electronegativity were also reported.[58] For instance,

$$\Lambda = \frac{0.75}{\chi_M - 0.25} \quad (7)$$

where χ_M is the Pauling electronegativity of the metal cation.

Yet another type of correlations is based on the so-called electronic polarizability of the oxygen atom ($\alpha_{O^{2-}}$) as a constituent of the metal oxide.[52]

$$\Lambda = 1.67\left(1 - \frac{1}{\alpha_{O^{2-}}}\right) \quad (8)$$

The polarizability of oxygen atom characterizes the ability of electrons involved in a chemical bond to move away from the ionic nucleus under the action of external electric field. It is calculated using the molar polarizability of the simple oxide

$$\alpha_m(A_iB_j) = i\alpha_A + j\alpha_B \quad (9)$$

where the subscripts A and B denote the cation and anion, respectively; and i and j are the corresponding stoichiometric coefficients. The molar polarizability of an oxide can be calculated by the Lorentz–Lorenz equation (Clausius–Mossotti relation)[52,59]

$$\alpha_m = \frac{3V_m}{4\pi N}\frac{n^2-1}{n^2+2} \quad (10)$$

where V_m is the molecular volume, N is the Avogadro constant and n is the refractive index.

These expressions were obtained using the experimentally measured optical basicity values of oxide glasses and are therefore of limited use because, in particular, the Lewis acidities were calculated using the Pauling electronegativities for individual ions ignoring structural features of oxide compounds. Numerical values thus obtained are only suitable for compounds with ionic metal–oxygen bonds. The results of calculations using the molar polarizability values[60] are also valid only for ionic oxides, whereas for compounds with noticeable contribution of the covalent component to the element–oxygen bond (d-metal oxides and oxygen compounds of nonmetals), the additivity of atomic polarizabilities [expression (9)] is violated.

The optical basicity characterizes the Lewis acidity in the bulk of the solid. However, in analyzing the gas–solid surface interaction one should know the actual Lewis acidity of the surface cations that directly interact with gas

molecules. It is believed[54] that for oxide systems with pronounced anisotropy of the crystal structure (*e.g.*, a layered structure), the bulk value of the optical basicity can be used to predict the reactivity of the surface. For oxides with dense crystal structures (*e.g.*, NiO or Co_3O_4), processes related to recovery of the surface may strongly influence its acidity. In this case, the so-called 'surface' optical basicity (Λ_s) should be used. For instance, the Λ_s value for nickel oxide can be determined using the electronic polarizability of oxygen atoms on the surface of the crystal, which is calculated using expression (8).[61] Equation (8) with inclusion of a correction computed using the polarizabilities of surface oxygen atoms,

$$\Lambda_s = \Lambda_b + 0.12 \qquad (11)$$

where Λ_b is the bulk optical basicity, can also be applied to other oxides with dense structure, *e.g.*, Al_2O_3 and MgO.

This approach allows one to predict the Lewis acidity of the oxide surface based on the chemical composition and crystal structure of oxide materials. However, it ignores the surface morphology, which often depends on the chemical prehistory of the material, in particular, on the method of synthesis, and thus still remains of limited use.[57]

3. The Sanderson electronegativity concept

The acid-base properties of metal oxide surfaces can be assessed using the Sanderson electronegativities.[62, 63] According to Sanderson, ionic and covalent bonds between different-nature atoms within the same compound do not complement one another, being mutually dependent components. For instance, consider two interacting atoms. If the oxidation state of one atom increases, the ionic component of the chemical bond increases, whereas the covalent component decreases due to redistribution of the electron density between the atoms in such a manner that the overall electronegativity within the compound stays unchanged. This is the principle of electronegativity equalization. Thus, the electronegativity of a chemical compound is the geometric mean of the individual electronegativities of the constituent atoms.

Following Sanderson, one can calculate partial atomic charges that characterize the contributions of the ionic component to the chemical bond using the cation electronegativities

$$q_M = \frac{\left[(\chi_M)^x(\chi_{Ch})^y\right]^{1/(x+y)} - \chi_M}{(\chi_M)^{1/2.08}} \qquad (12)$$

where q_M is the partial charge on the cation, χ_M is the cation electronegativity, χ_{Ch} is the chalcogenide electronegativity (for oxygen, $\chi = 3.61$), and x, y are the stoichiometric coefficients of the compound.

To date, numerical values present in Eqn (12) are known for a large number of cations in different formal oxidation states. This enables classification of corresponding oxides with respect to their Lewis acidity values,[64] which are determined as the differences between the formal oxidation state of the cation and the doubled partial charge q_M. This method for calculations of bond ionicities and partial charges on atoms that form solids with atomic lattices is simple and therefore widely used to compare the reactivities of same-type materials, most often, zeolites that are utilized as catalysts.[65, 66]

More recently, the Sanderson principle of electronegativity equalization was significantly extended to enable calculations of partial charges on atoms in the structure of solids using the lattice parameters, atomic coordinates and the Sanderson electronegativities of the chemical elements. To this end, a method based on the density functional theory was adapted;[67] it allows one to calculate the distribution of partial atomic charges and to assess their acidity, as well as to reveal differences between structurally non-equivalent atoms of the same element, which can act as active adsorption sites on the surface of materials.

It should be noted that metal oxide surfaces exhibit not only Lewis acidity, but also Brønsted acidity, the latter being characterized by the ability to donate protons in the interaction with bases. The Brønsted acidity emerges as a result of dissociative adsorption of water molecules with the formation of hydroxyl groups (water is almost always present on the surface of metal oxides). The strength of such acid centres is determined by the deprotonation energy which can be evaluated from quantum chemical calculations.[68–70] Even simpler calculations using the Sanderson electronegativities are often performed for catalysts that were used to demonstrate linear correlations between the strength of Brønsted acid sites and partial charges on atoms — both oxygen anions and cations,[67]

$$pK_{aO} = -42.2\,q_O - 19.8 \qquad (13)$$

where pK_a is the theoretical acidity constant.

4. Reactions of gases on oxide surfaces

Oxide materials have found applications in heterogeneous catalysis; in particular they are utilized as inert supports for catalysts of acid-base transformations of gas molecules (polycondensation, esterification, polymerization reactions, *etc.*). These materials are most widely used as catalysts of both partial and complete oxidation of organic compounds in air. Taking into account the fact that in sensors, gas–solid interactions mainly occur in air, it is the redox reactions on the surface of semiconductor metal oxides (in particular, nanocrystalline SnO_2) involving gas molecules that make the major contribution to the formation of sensor response.

Two types of species are involved in the oxidation of adsorbed molecules on oxide surfaces. These are various forms of chemisorbed oxygen, including hydrated oxygen (OH groups), and anions occupying lattice sites in the crystal structure of SnO_2.[71, 72] Chemisorbed oxygen, in the form of molecular or atomic ions, represents highly reactive electrophilic species that readily interact with almost all adsorbed molecules. Lattice oxygen is considered a less reactive nucleophilic form of the oxidant.[73] We will discuss modern approaches to prediction of the reactivity of the surface of oxide materials in the redox reactions with gas molecules based on the chemical composition and structure of oxides.

Oxidation of molecules adsorbed on idealized oxide surface represented by metal cations M^{n+} and oxygen anions O^{2-} occupying lattice sites is due to lability of nucleophilic anions, which can attack the adsorbed molecules, breaking the existing chemical bonds in these mole-

cules and forming new bonds. The adsorption of gas molecules, which occurs with partial transfer of electron density to the metal cation on the surface, leads to activation of these molecules, *viz*., creation of additional centres with a partial positive charge, which later may become centres for nucleophilic attack by the lattice anions O^{2-}. In essence, activation of adsorbed molecules is a kind of acid-base chemisorption interaction; that is why the qualitative and quantitative composition of the final products of gas–solid redox interaction can be governed by the acidity of the surface.[74] This mechanism of oxidation on metal oxide surfaces was initially proposed by Mars and van Krevelen.[75] More recently, it was substantiated for a large number of oxide systems[76,77] using kinetic[78] and direct methods of investigation of the structure of oxide surfaces.[79] As a result, the oxide surface goes to the so-called reduced state that is characterized by a large number of oxygen vacancies and metal cations in lower oxidation states compared with the cations in the bulk material.

If the gas phase contains oxygen, re-oxidation of the surface occurs. It involves adsorption of molecular oxygen, its dissociation and incorporation of anions into positions of oxygen vacancies in accordance with the following equations

$$O_{2(gas)} \longrightarrow O_{2(ads)} \tag{14}$$

$$O_{2(ads)} + e^- \longrightarrow O^-_{2(ads)} \tag{15}$$

$$O^-_{2(ads)} + e^- \longrightarrow 2\,O^-_{(ads)} \tag{16}$$

$$O^-_{(ads)} + e^- \longrightarrow O^{2-}_{(ads)} \tag{17}$$

$$O^{2-}_{(ads)} \longrightarrow O^{2-}_{(cryst)} \tag{18}$$

Here $O_{2(gas)}$ is the oxygen molecule in the gas phase; $O_{2(ads)}$ is the adsorbed oxygen molecule; $O^-_{2(ads)}$, $O^-_{(ads)}$ and $O^{2-}_{(ads)}$ are respectively the molecular ionized, atomic ionized and doubly ionized atomic forms of oxygen chemisorbed on the oxide surface; and $O^{2-}_{(cryst)}$ is the oxygen anion occupying a lattice site in the crystal structure of the material.

The possibility for this chemical cycle to occur predetermines a wide use of oxide materials in heterogeneous catalysis of the oxidation of, mainly, organic substances.[80] Such a redox interaction is also immediately related to sensor materials. As follows from Eqns (14)–(18), in the case of SnO_2-based materials this interaction can be accompanied by much more pronounced changes in the electron density in the conduction band compared to adsorption interaction with the gas phase (this interaction is a kind of acid-base interaction). Because of this, classification of the metal oxides capable of being modifiers of the surface of nanocrystalline SnO_2 with respect to their activity in the redox interaction with gas molecules seems to be of great importance.

Various attempts to classify metal oxides with respect to their reactivity in the interaction with gas molecules for the Mars–van Krevelen mechanism depending on their chemical composition and structure as well as on the nature of the oxidized molecules have been reported to date. An example is provided by the classification[81] based on the properties that seemingly determine the rates of consecutive activation of adsorbed molecule, its reactions with a labile form of lattice anion O^{2-} and subsequent recovery of the active site, *i.e*., compensation of the surface species O^{2-} consumed in the course of dissociative adsorption of oxygen. The first process depends solely on the oxide surface acidity determined by the electronegativity of cations in the near-surface levels of the oxide lattice (see above). The activity of the oxidation of the activated molecule

$$M^{n+}-O^{(2-x)-} + R \longrightarrow M^{(n-x)+} + RO^{2-} \tag{19}$$

depends on the strength of the metal–oxygen bond, which for the bulk material can be estimated from the standard enthalpy of formation of the oxide. The authors[81] assumed that the rate of regeneration of the oxidation centre on the surface in the reaction

$$M^{(n-x)+} + \frac{x}{4}O_2 \longrightarrow M^{n+} + \frac{x}{2}O^{2-} \tag{20}$$

is determined by a combination of properties, namely, the surface acidity and the energy of the metal–oxygen bond.

Unfortunately, this thermodynamical approach to prediction of the redox activity of oxide surfaces failed to reveal correlations with the real catalytic activity of oxide compounds even in very simple transformations. The reason for the failure of this, at first glance a promising concept, was a large number of additional factors influencing the course of heterogeneous redox reactions, which were ignored in the proposed scheme of oxidation.

According to Eqns (14)–(18), electrophilic chemisorbed anions O^-_2, O^{2-}_2 and O^- (see Ref. 82) may appear on the oxide surfaces; these species can form during reversible adsorption of molecular oxygen on the oxide surface irrespective of the redox processes proceeding by the Mars–van Krevelen mechanism. This may lead to the occurrence of surface oxidation reactions that are not subject to this mechanism.[83]

There are several forms of oxygen that can participate in redox reactions. Consider the following ionized forms: O^-_2, O^{2-}_2, O^- and O^{2-}, ignoring radicals and ozone-like species (as far as we know, no publications concerning the involvement of such species in reactions on oxide surfaces have been reported so far). According to the energy diagram shown in Fig. 5, the higher the charge of the ionized form of oxygen the lower its stability in the gas phase.

The O^-_2 species is the only ionized form of oxygen in the gas phase which is energetically more favourable than the electrically neutral molecular form. Electrostatic interaction of O^-_2 with ions on the oxide surface can additionally stabilize the species. The O^{2-} anion can be stabilized on the surface only in the position of the oxygen vacancy. The numerical values listed in the energy diagram are approximations because the exact positions of ionized oxygen atoms adsorbed on the surface and their environment are hard to predict.

It was proposed[73] to divide oxides into three main groups with respect to type of the most abundant anions adsorbed on the surface. To this end, an original method based on iodometric titration was developed. The technique allows one to determine the change in the oxidation state of cations in the oxide upon adsorption of oxygen on the oxide surface.[84] The additional positive charge acquired by cati-

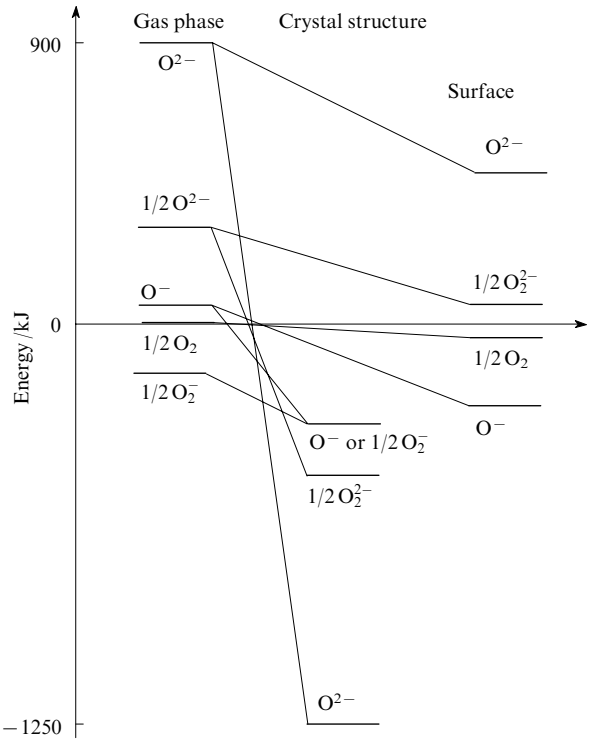


Figure 5. Energy diagram for different oxygen species in the gas phase, in the solid phase and on the surface of binary oxide MO.[73]

ons in the course of adsorption is compared with the negative charge acquired by the oxygen species adsorbed on the surface. The experimental procedure makes it possible to determine the amount of oxygen adsorbed on the surface and thus to evaluate the specific negative charge, which in turn will allow one to establish the predominant form of chemisorbed ionized species on the surface, namely, O^-, O_2^- or O^{2-}.

The first group includes oxides with p-type conductivity, namely, NiO, MnO, CoO and Co_3O_4. In this case, metals go to higher oxidation states with relative ease and therefore more readily donate the electron density to the adsorbed oxygen species with higher electronegativity. At room temperature and in the presence of excess oxygen, the surface of this group of oxides is rapidly covered with a large number of electrophilic anions O^- and O_2^-. As the temperature of the surface increases, the rate of dissociative adsorption of oxygen increases and adsorbed O^{2-} species appear; their proportion increases. The surface thus becomes negatively charged and the corresponding ion–ion electrostatic interaction causes diffusion of metal cations from the bulk towards the surface and their involvement in the formation of new crystallographic planes with participation of adsorbed anions O^{2-}.

The second group of metal oxides includes ZnO, TiO_2, and SnO_2. They also can donate the electron density to the adsorbed oxygen molecules; in this case, the excess electron density is primarily due to nonstoichiometry with respect to oxygen. This group of oxides differs from the first group by a relatively small number of active surface sites suitable for being utilized in electron density transfer to the adsorbed oxygen molecules. In the case of non-stoichiometric semiconductors, an important role is played by the surface oxygen vacancies. They can be the sites of reversible adsorption of oxygen resulting in O^{2-} anions that form strong chemical bonds with the cationic environment of the vacancy only after heat treatment (>700 °C) in the presence of excess oxygen. Because of this, the nature and structural features of defects on the surface of such materials including nanocrystalline SnO_2 can play a decisive role in the interaction with gas molecules, which actually occurs at much lower temperatures.

The third group of oxides includes molybdenum, tungsten, vanadium oxides and other oxides of transition metals in higher oxidation states. These compounds cannot donate the electron density to the adsorbed oxygen molecules; therefore, no stable adsorbed electrophilic ionized forms of oxygen are formed on the stoichiometric surfaces of these oxides. Electrophilic species formed on the reduced surface are transformed to the nucleophilic species O^{2-} and occupy positions of oxygen vacancies in the crystal structure. Oxidation of gases on the surfaces of the oxides in question can be quite rigorously described in terms of the Mars–van Krevelen mechanism. These oxides are often used as catalysts for partial oxidation of hydrocarbons and other classes of organic compounds.

This classification ignores main-group metal oxides whose cations can exist in a single oxidation state and therefore exhibit no electron-donating properties. Utilization of such oxides as oxidation catalysts requires additional efforts aimed at creating defects in their crystal structures[85] and, correspondingly, oxygen vacancies on the surface to play the role of adsorption sites and to form electrophilic active oxygen species.

Detailed studies on the mechanisms of formation and reactivity of electrophilic forms of adsorbed oxygen on oxide surfaces are scarce.[82] It is believed that these species are more reactive than the nucleophilic lattice anions O^{2-} and have higher mobilities.[72] Also, they can act as adsorption sites and serve for activation of molecules on the surface. Taking into account this fact, the first group of oxides and materials based on them are most often used as catalysts for complete and non-selective oxidation of adsorbed molecules.[74,86] The role of adsorbed electrophilic ions O^- in selective oxidation was also pointed out.[87,88]

To date, qualitative concepts underlying modern approaches to the design of oxide materials with specified reactivities have been developed. These concepts include criteria for the choice of the chemical composition of bulk oxide materials and methods for modification of their surfaces or crystal structures to vary the reactivity of lattice oxygen atoms in the redox processes.

In the text below, we will discuss the applicability of the concepts outlined above for prediction of the reactivity of metal-oxide semiconductor sensor materials in reactions with gases and as well as relationships between the reactivity and actual sensor sensitivity of these materials.

III. Effect of modifiers on the sensing properties of nanocrystalline tin dioxide

This Section is devoted to analysis of experimental results obtained in studies on the sensing properties of modified

SnO_2. The main idea of these studies is to modify the SnO_2 surface to increase the proportion of a particular type of adsorption sites to ensure more selective interaction with the gas phase. A modifier introduced into the structure of a nanocrystalline metal oxide influences the chemical composition, microstructure, surface state, electrical properties and reactivity of the oxide. The structure of the modified nanocrystalline SnO_2 and the distribution of the modifier between the bulk and surface of nanocrystalline grains have been discussed.[21]

The modifier influence on the nature and concentration of chemisorbed oxygen on the SnO_2 surface is considered below. The concentration of oxygen in air is rather high and varies around 20.5 vol.%. On the one hand, oxygen adsorbed on the surface of semiconductor oxides determines the height of the Schottky barrier on the grain boundaries. On the other hand, adsorbed oxygen participates in the surface reactions. Generally, there is a power law relationship between the sensor signal and the partial pressure of the gas to be detected; in addition, the power law exponent is specific to the predominant type of the chemisorbed oxygen species.[89] Thus, parameters describing the interaction of the sensor material with oxygen are of crucial importance for the design of highly sensitive gas sensors.

1. Types of oxygen species chemisorbed on SnO_2 surface

Experimental studies of the interaction of SnO_2 with oxygen as well as corresponding model calculations have been well documented (see, *e.g.*, Refs 10 and 90–94). In the temperature interval from 100 to 500 °C, *i.e.*, in the operating temperature range of resistive gas sensors, the saturated vapour pressure of oxygen over solid SnO_2 is $\sim 10^{-28}-10^{-26}$ atm.[95] Therefore, the conductivity of nanocrystalline materials in air is determined by different types of oxygen species adsorbed on the surface of semiconductor grains rather than by the concentration of oxygen vacancies in the oxide structure. In this temperature interval, the interaction of atmospheric oxygen with the surface of n-type semiconductor oxides results in the formation of molecular and atomic chemisorbed oxygen species $O^-_{2(ads)}$, $O^-_{(ads)}$ or $O^{2-}_{(ads)}$. The results of studies on this interaction obtained by oxygen TPD, IR spectroscopy and electron paramagnetic resonance were summarized in reviews.[92,93] It was shown that molecular ions O^-_2 predominate at temperatures <150 °C. At higher temperatures, the formation of monatomic ions O^- and O^{2-} is suggested. Generally, chemisorption of oxygen on the surface of an n-type semiconductor oxide can be described as follows [10]:

$$\frac{\beta}{2}\,O_{2(gas)} + \alpha\,e^- + D \rightleftharpoons O^{-\alpha}_{\beta(ads)} \qquad (21)$$

where $O_{2(gas)}$ is the oxygen molecule in the gas phase; e is an electron which can reach the surface, *i.e.*, its energy is high enough to overcome the barrier produced by the negatively charged surface (the concentration of such electrons is $n_s = [e]$); D is an unoccupied surface site for chemisorption of oxygen; $O^{-\alpha}_{\beta(ads)}$ is the chemisorbed oxygen species ($\alpha = 1$ and 2 for the singly and doubly ionized species, respectively); $\beta = 1$ and 2 for the atomic and molecular species, respectively.

Initially (electrically neutral surface), adsorption is limited by the chemical factor, namely, the activation energy of adsorption and dissociation. As the surface charge appears, a limitation is produced by the potential barrier that precludes the motion of electrons from the bulk to the surface. The activation energy of desorption remains unchanged in the course of the process provided that the surface area is large enough to exclude the interaction between the adsorbed species. The activation energies of adsorption and desorption are included in the corresponding constants $k_{(ads)}$ and $k_{(des)}$.[10]

Using the mass action law, from Eqn (21) one gets

$$k_{(ads)}\,[S]\,n_s^{\alpha}\,p_{O_2}^{\beta/2} = k_{(des)}\,[O^{-\alpha}_{\beta(ads)}] \qquad (22)$$

where $[S]$ is the total concentration of the available surface sites for oxygen adsorption.

A relation between the electron concentration (n_s) and the partial pressure of oxygen in the gas phase has the form [96]:

$$\log n_s = \mathrm{const}_1 + \log\left(1 - \frac{n_s}{n_b}\right) - m \log p_{O_2} \qquad (23)$$

where n_b is the charge carrier concentration in the bulk of the material and $m = 1$, 0.5, 0.25 for O^-_2, O^- and O^{2-}, respectively.

If the sensor represents a porous layer (a thick film formed by small crystallites), its conductivity is proportional to n_s (see Ref. 10)

$$\sigma \sim n_s \qquad (24)$$

and Eqn (23) can be transformed to

$$\log \sigma = \mathrm{const}_2 + \log\left(1 - \frac{\sigma}{\sigma_0}\right) - m \log p_{O_2} \qquad (25)$$

where σ is the material conductivity at a given partial pressure of oxygen and σ_0 is the material conductivity at $p_{O_2} \to 0$.

Thus, assuming that σ_0 equals the conductivity of the sensor material in, *e.g.*, pure argon (oxygen content is at most 2 ppm), one can experimentally determine the value

$$\log\left(1 - \frac{\sigma}{\sigma_0}\right)$$

at any partial pressure of oxygen in the gas. Using the linear dependence of the conductivity on the partial pressure of oxygen in the coordinates

$$\left[\log \sigma - \log\left(1 - \frac{\sigma}{\sigma_0}\right)\right] \propto \log p_{O_2}$$

one can assess the type of the predominant species of chemisorbed oxygen.

At 200 °C, chemisorption of oxygen on the surface of unmodified SnO_2 mainly occurs with the formation of

molecular species $O^-_{2(ads)}$ ($m \approx 1$).[96] Raising the temperature causes an increase in the proportion of monatomic species $O^-_{(ads)}$, as indicated by the decrease in the coefficient m. As the crystallite size increases, the effect becomes more pronounced.

At 200 °C, modification of SnO_2 has little effect on the predominant form of chemisorbed oxygen, *viz.*, chemisorption mainly occurs with the formation of the molecular form $O^-_{2(ads)}$ irrespective of the type of modifier ($m \approx 1$). At higher temperatures (300–350 °C), the m value decreases, thus indicating an increase in the content of the monatomic species $O^-_{(ads)}$. The effect of the modifier nature on the type of the predominant form of chemisorbed oxygen becomes more pronounced in the following order of oxides:

Fe < In < La < Ru < Ni < Pd < Pt.

This is consistent with an increase in the optical basicity (reduction of Lewis acidity) of the modifier cations (Fig. 6). Thus, the approaches described above are suitable for qualitative assessment of the effect of modifiers on the oxidation properties of SnO_2 surface.

A greater body of information on the redox activity of materials and its nature can be obtained using temperature-programmed reduction of materials with hydrogen (H_2-TPR).[97] The H_2-TPR profiles of materials based on SnO_2 (Fig. 7) demonstrate two clearly seen maxima, one in the low-temperature interval (100–350 °C) and the other, more pronounced, in the high-temperature interval (380–660 °C). The high-temperature peak corresponds to reduction of the material to metallic tin; the low-temperature maximum characterizes reduction of the surface, *i.e.*, hydrogen consumption by various chemisorbed oxygen species or by lattice oxygen.

It should be noted that two types of lattice oxygen atoms, *viz.*, three-coordinate and two-coordinate (bridging) ones, can exist on the $SnO_2(110)$ crystallographic plane. Reduction of the surface manifests itself as an increase in the number of lattice oxygen vacancies occupying the bridging oxygen sites. Correspondingly, some tin cations in the +4 oxidation state with six oxygen atoms in the coordination environment in the near-surface layer become tin cations in the oxidation state +2 with four oxygen atoms in the coordination sphere. A low-temperature shoulder of the high-temperature absorption maximum characterizes partial transformation of SnO_2 to SnO, followed by complete reduction to metallic tin. Reduction to the intermediate state is ensured by a high proportion of surface O^{2-} anions; their loss in the course of reduction is compensated by ion transport from the bulk of the semiconductor material grains. An increase in the SnO_2 crystallite size causes an abrupt decrease in the proportion of surface oxygen atoms, as indicated by a decrease in the low-temperature peak. At the same time, the shoulder near the

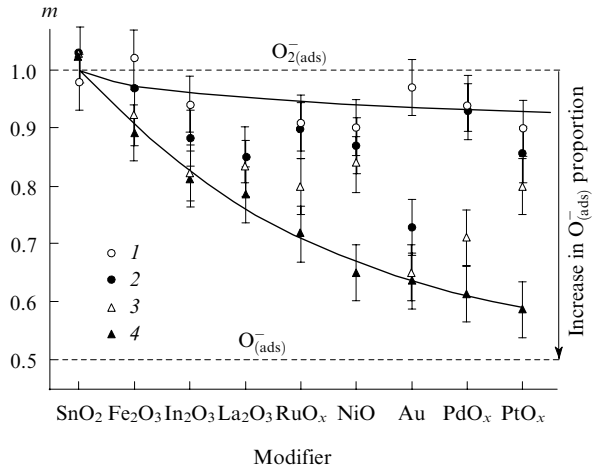


Figure 6. Correlation between calculated values of the coefficient m in Eqn. (25) for pure and modified SnO_2 and the acidity of the modifier cation M^{n+} (see Ref. 71).
T/°C: 200 (*1*), 250 (*2*), 300 (*3*) and 350 (*4*); oxides are arranged in order of increasing cation acidity.

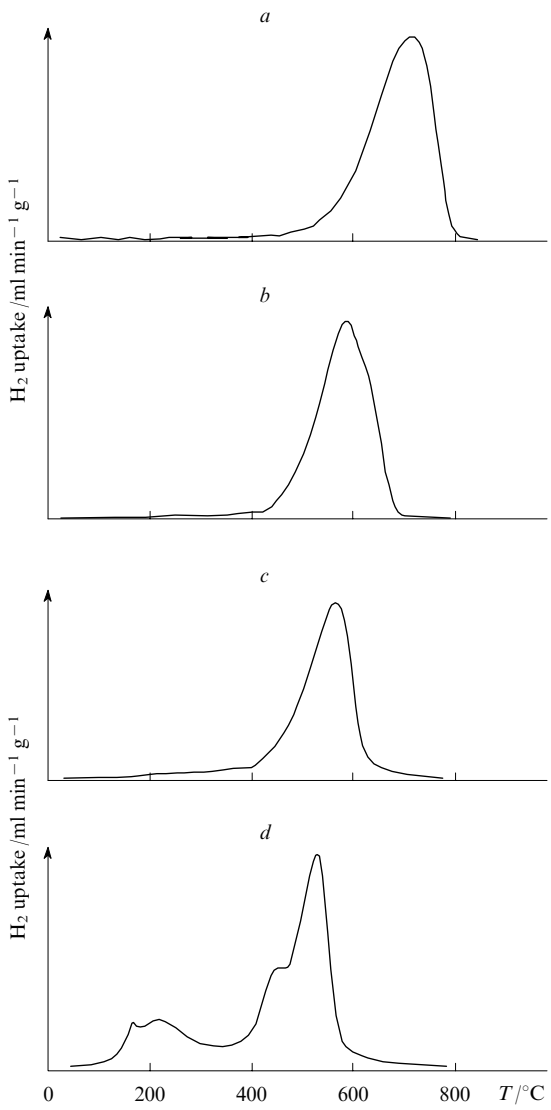


Figure 7. H_2-TPR profiles for nanocrystalline SnO_2 surfaces with different grain size.[98]
Single crystal (*a*); grain size /nm: 22 (*b*), 9 (*c*) and 4 (*d*).

high-temperature maximum almost disappears and becomes shorter; this suggests simultaneous occurrence of two processes, reduction of the oxide matrix to SnO and to metallic tin. In addition, materials with grains larger than 20 nm in size exhibit a high-temperature shoulder near the high-temperature peak. Probably, partial transition of the material to the metallic state causes the appearance of additional diffusion barriers in the near-surface layer; these barriers preclude the motion of oxygen anions from the bulk material to the surface.

For Ru-, Pt- and especially Pd-modified materials, the high-temperature maximum is shifted to the low-temperature region (Fig. 8). This can be due to the catalytic activity of noble metal clusters in the nanocrystalline SnO_2 matrix. The most probable mechanism of this process involves mutual spillover of hydrogen and lattice oxygen present in the SnO_2 matrix through the Pd or PdO_x clusters.[99] Spillover of molecular hydrogen means that hydrogen molecules dissociate on palladium clusters, migrate towards oxygen species chemisorbed on the surface and react there. Chemisorbed oxygen species appear on the surface of Pd clusters because atmospheric molecular oxygen can be adsorbed on this surface and then dissociate. Examples illustrating this mechanism of the interaction with the gas phase in the systems $Rh-TiO_2$, $Rh-Al_2O_3$, $Rh-CeO_2$, $Rh-SiO_2$, $Pt-Al_2O_3$, $Pd-Al_2O_3$ and $Pd-Mn_2O_3$ are documented.[99] In addition, an oxygen isotope exchange study[100] revealed that modification of nanocrystalline SnO_2 with palladium leads to a multistep heteroexchange mechanism involving dissociation of O_2 molecule on the surface of palladium clusters, spillover of atomic oxygen from Pd clusters to the SnO_2 surface and subsequent exchange of atomic oxygen species with lattice oxygen. It should be noted that the last-mentioned process is reversible and can be reversed under favourable conditions.†

For all materials, the high-temperature peak appears at similar temperatures (~ 420 °C), thus corresponding to the energy barrier to oxidation by the Mars–van Krevelen mechanism.[97]

The concentration of oxygen adsorbed on the SnO_2 surface (4-nm tin dioxide grains) estimated from H_2-TPR data for the interaction

$$O^-_{2(ads)} + 2\,H_2 \longrightarrow 2\,H_2O + e^- \qquad (26)$$

is $\sim 10^{-5}$ mol m^{-2}, or 5×10^{-2} monolayer. According to Weisz limitation,[9] this corresponds to the upper bound of the coverage density of the semiconductor surface with charged species under the equilibrium ion sorption conditions.

In most cases, modification of SnO_2 surface leads to a decrease in the amount of hydrogen absorbed at low temperatures. This is an indirect indication of an increase in the proportion of the monatomic chemisorbed oxygen species O^- on the surface. Indeed, having compared reactions (26) and

$$O^-_{(ads)} + H_2 \longrightarrow H_2O + e^- \qquad (27)$$

for the surfaces bearing equal negative charges due to the presence of chemisorbed oxygen species, one can suggest that in the latter case, a less intense absorption of hydrogen should be observed.

Additional information on the concentration of the most mobile and reactive oxygen species on the SnO_2 surface can be extracted from H_2-TPR data for the materials pre-treated in oxygen-free nitrogen atmosphere. Chemical inertness of molecular nitrogen rules out the possibility of reduction of the SnO_2 surface. At the same time, close size and polarizability values of the nitrogen and oxygen

† This process can be called 'reverse spillover'.

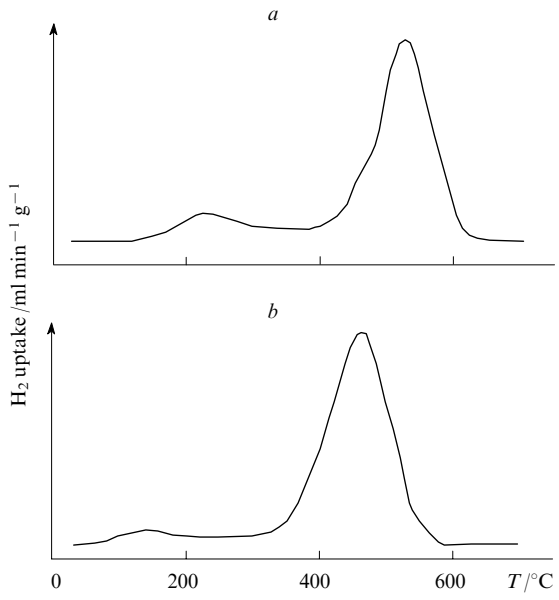


Figure 8. Shift of hydrogen uptake peaks in the course of H_2-TPR experiment upon modification of nanocrystalline SnO_2 with Pd catalytic clusters.
Sample: untreated (*a*) and modified (*b*).

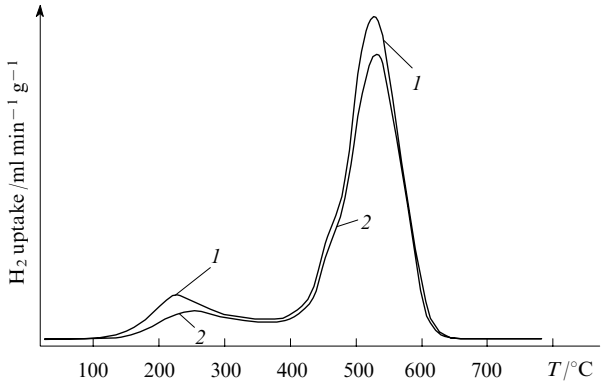


Figure 9. Effect of pre-treatment of nanocrystalline SnO_2 surface (4-nm grains) on the H_2-TPR profile.[71]
Pre-treatment in air (*1*) and in N_2 stream (*2*).

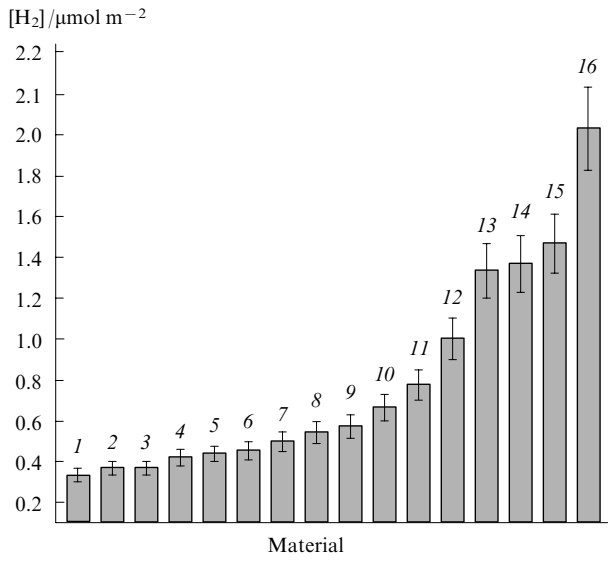


Figure 10. Amount of hydrogen consumed by oxygen species on the surface sensor materials based on chemically modified nanocrystalline SnO_2 (according to H_2-TPR data).[71]
Material: NiO–Au-350/SnO_2 (*1*), Pt-500/SnO_2 (*2*), SnO_2-500 (*3*), Pt-500/SnO_2 (*4*), Au-300/SnO_2 (*5*), MoO_3-500/SnO_2 (*6*), SnO_2–V_2O_5-500/SnO_2 (*7*), SnO_2–Cr_2O_3-300/SnO_2 (*8*), SnO_2-700 (*9*), RuO_x-300/SnO_2 (*10*), PdO_x-300/SnO_2 (*11*), SnO_2-300 (*12*), Fe_2O_3-500/SnO_2 (*13*), Ru-700/SnO_2 (*14*), Cr_2O_3-500/SnO_2 (*15*) and PdO_x-500/SnO_2 (*16*).

molecules enable a competition for adsorption sites on the SnO_2 surface.[73] If nanocrystalline SnO_2 obtained by annealing β-$SnO_2 \cdot n\,H_2O$ gel at 300 °C (SnO_2-300) is pre-treated in nitrogen, both peaks in the TPR profiles weaken (Fig. 9). This indicates desorption of the oxygen species with the highest mobility from the SnO_2 surface; the process is to some extent redeemed by the delivery of O^{2-} anions from the bulk. The concentration of such oxygen species on the surface of untreated and modified SnO_2 can be determined taking into account differences between corresponding H_2-TPR profiles.

The maximum concentration of mobile oxygen species was found for SnO_2 modified with Pd and Cr_2O_3 (Fig. 10). In both cases, this can be due to an increase in the oxidation state of the modifier, namely, by partial oxidation of palladium clusters to PdO_x and formation of Cr=O groups with transition of the surface chromium cation to a higher oxidation state Cr^{4+}. Correspondingly, these materials are expected to exhibit the highest activity and sensor sensitivity in the oxidation of gas molecules at the surface.

2. Classification of gases

Preliminary choice of modifiers in order to design selective and highly sensitive materials can be done based on analysis of the properties of molecules of the gas to be detected. Gases can be classified using appropriate properties of their molecules, *e.g.*, the ionization potential, electron affinity and proton affinity (Fig. 11). To begin with, all gases are divided into oxidizing and reducing gases. Oxidizing gases include gases that exhibit electron-withdrawing properties; adsorption of oxidizing gases leads to a decrease in the concentration of charge carriers in the near-surface layer of

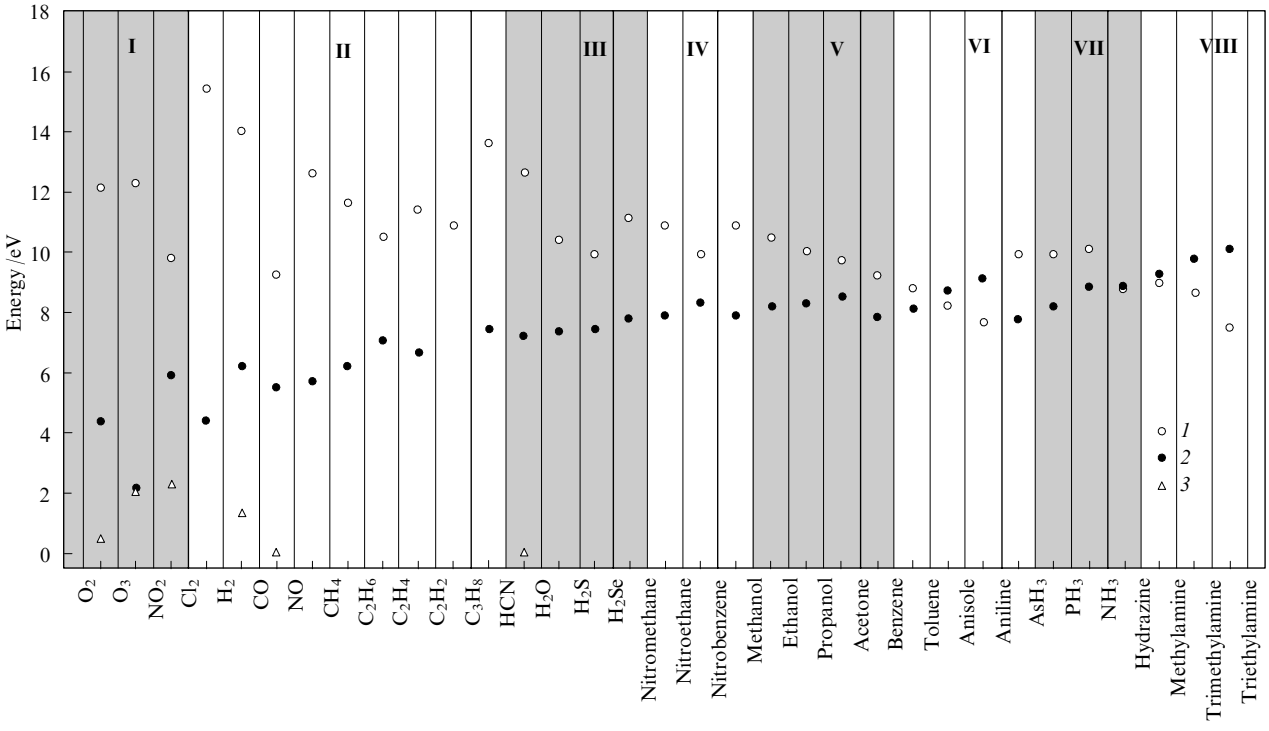


Figure 11. Energy parameters of molecules in the gas phase.[101] Ionization potential (*1*), proton affinity (*2*) and electron affinity (*3*).

n-type semiconductor oxides. This group may include gases whose molecules are characterized by high electron affinity and high ionization potential (group I in Fig. 11), *viz.*, oxygen, nitrogen dioxide, ozone and chlorine.

Reducing gases include gases that are oxidized upon the interaction with the surface of sensor materials. In the case of n-type semiconductor oxide, the concentration of charge carriers in the near-surface layer of the semiconductor increases. The mechanism of chemical interaction of the reducing gases and, therefore, the mechanism of the sensor response depend strongly on the reducing power of the gas. Gases that exhibit the properties of weak electron donors and whose molecules have rather low proton affinities, in particular, CO, H_2, saturated hydrocarbons (group II in Fig. 11) are oxidized in the interaction with the chemisorbed oxygen species at the surface of the sensor material. Adsorption of typical acids (group III) or bases (groups VII, VIII) on the surface of sensor materials may involve not only oxidation reactions, but also an additional donor-acceptor interaction. Processes with participation of complex organic molecules (groups IV–VI) may follow different paths depending on the concentration of basic and acidic adsorption sites of different strength on the semiconductor surface.

Viability of the concept of directed modification of SnO_2 to enhance the sensor sensitivity was tested using typical representatives of different groups including NO_2 (group I), CO (group II), NH_3 (group VII), H_2S (group III), acetone and ethanol (group V).

3. Sensing properties of modified tin dioxide towards simple reducing gases taking CO as an example

A correct comparison of the sensing properties of metal-oxide semiconductor materials from the standpoint of chemical materials science is often a complicated task. The prehistory of materials having the same chemical composition may strongly influence the reactivity of their surfaces and, therefore, the sensing properties. In this review, we thoroughly considered the sensor materials synthesized by the sol–gel method and subsequently impregnated with modifiers; the only exception is Au–SnO_2, namely, gold was introduced into the structure of the material by anionic adsorption.[24] The structures of such materials were analyzed in reviews (see, *e.g.*, Ref. 21). Here, mention may only be made that modification of the structure of nanocrystalline SnO_2 with platinum group metals is accompanied by the formation of partially oxidized clusters of these metals on the surface of nanocrystalline SnO_2 grains. Gold utilized as modifier is distributed across the surface in the form of catalytic clusters. Other modifiers considered here can form catalytic clusters on the surface of semiconductor grains or form solid solutions with SnO_2. Depending on the heat treatment conditions of the material and on the content of modifier, the modifier can exist in two forms (catalytic clusters and solid solution) simultaneously. In addition, the heat treatment temperature of the material obtained by the sol–gel method governs the surface morphology and microstructure and therefore often strongly influences the sensing properties. In this connection, the synthesis temperature is indicated when necessary in addition to the chemical composition of materials based on the modified nanocrystalline SnO_2.

Primarily, the mechanism of CO interaction with the metal oxide surface is temperature dependent.[102, 103] The carbon monoxide molecule can act as both electron donor and acceptor. It can interact with acid surface sites (coordinatively unsaturated metal cations, Lewis acids) and with oxygen ions representing the Brønsted or Lewis bases.

The structure of CO molecular orbitals is such that electron density can be transferred from the CO molecule to unoccupied orbitals of metal (σ-donor) and from the metal d-orbitals to the unfilled antibonding orbitals of CO (π-acceptor).[103] At elevated temperatures, CO reacts with adsorbed or lattice oxygen on the oxide surface to give CO_2 as the final oxidation product.

Materials based on the modified SnO_2 demonstrate different temperature dependences of the sensor response (signal) towards CO (Fig. 12).[24, 104] Palladium-modified SnO_2 exhibits the maximum sensor signal at low measuring temperature (200 °C); the signal weakens as the measuring temperature increases.[105] All other materials considered in this Section show an increase in the signal in the presence of CO with increasing measuring temperature. This points to different mechanisms of formation of the sensor response.

The oxidation of carbon monoxide with chemisorbed oxygen is the main process responsible for the formation of the sensor response of SnO_2,[10]

$$\beta\,CO_{(gas)} + O^{-\alpha}_{\beta(ads)} \longrightarrow \beta\,CO_{2(gas)} + \alpha\,e^- \qquad (28)$$

where $CO_{(gas)}$ is the CO molecule in the gas phase, $O^{-\alpha}_{\beta(ads)}$ is the chemisorbed oxygen species, e^- is an electron that passes to the conduction band as a result of the reaction and $CO_{2(gas)}$ is the reaction product molecule desorbed from the SnO_2 surface in the gas phase. Low-temperature sensitivity of the palladium-modified SnO_2 correlates with the presence of various reactive chemisorbed oxygen species (see above). Probably, at 200 °C, the oxidation of CO proceeds by the Eley–Rideal mechanism,[106] according to which CO molecules in the gas phase are oxidized by atomic oxygen species that are present on the solid surface. This requires approach of the reacting species, which can be represented as collision between the gas molecule and the active surface site. The lowest activation energy of the process was obtained[106] for the oxidation by $O^-_{(ads)}$ ion adsorbed on the PdO(100) surface; also, an oxygen vacancy in the structure of PdO in the immediate vicinity of the oxidant species additionally decreases the activation energy.

This oxidation mechanism requires 'turnover' of the oxidation sites, *i.e.*, filling of adsorption sites or surface oxygen vacancies that are formed as a result of reduction with partially oxidized palladium clusters. At low temperatures, this is possible due to so-called reverse spillover, *i.e.*, transfer of adsorbed electrophilic oxygen species present on the surface of the SnO_2 matrix to palladium clusters. It is this process leading to changes in the concentration of the adsorbed oxygen species on the semiconductor surface that is responsible for a relatively weak but reliably detected sensor response towards CO. Raising the temperature causes re-oxidation of the PdO_x surface at the expense of dissociation of molecular oxygen adsorbed from the gas phase. As a result, the oxidation of CO is fully located on catalytic clusters. Oxidation has no effect on the concentration of charge carriers in the conduction band of the semiconductor oxide matrix; therefore, the sensor response towards CO abruptly decreases.

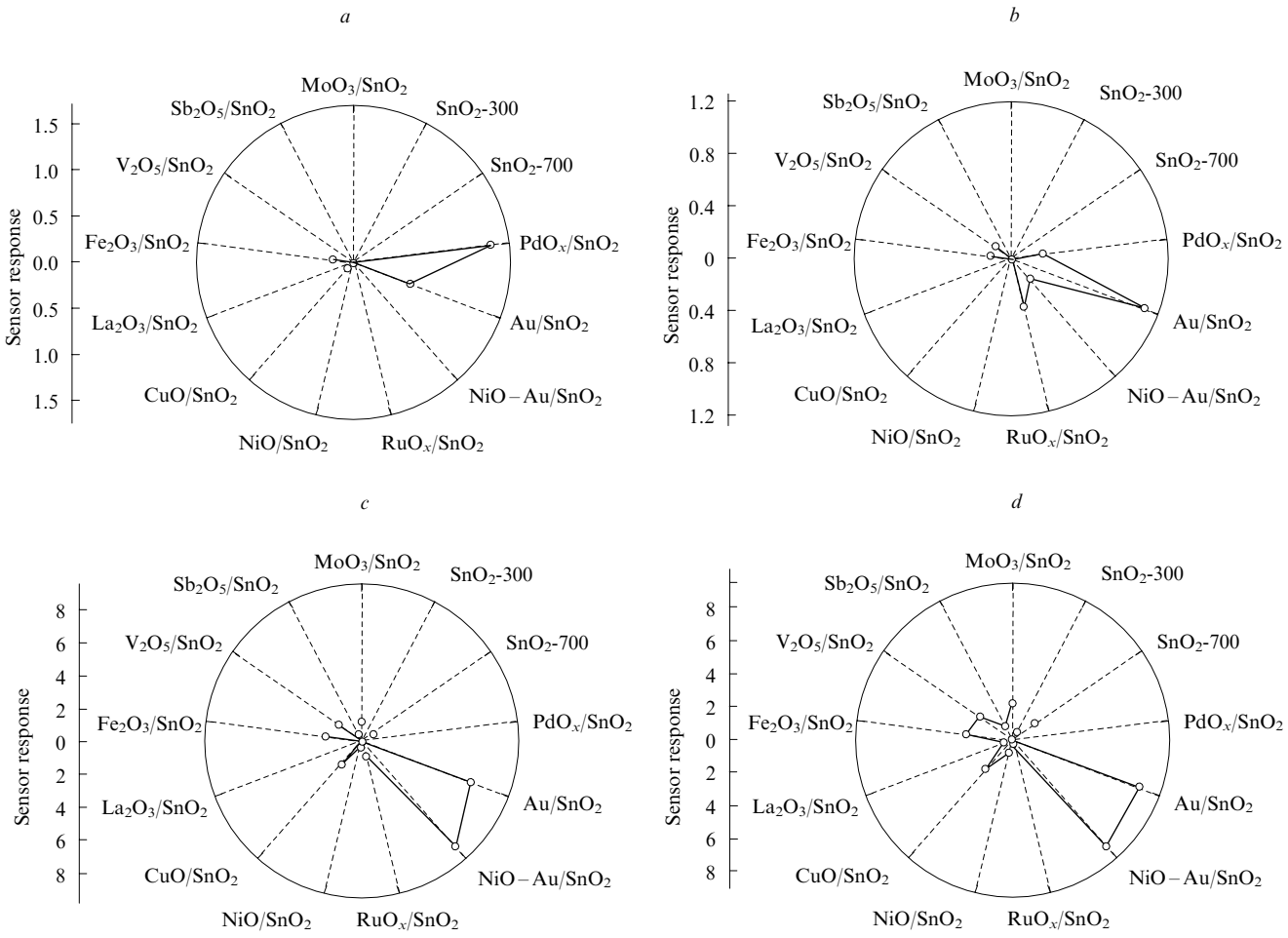


Figure 12. Sensitivity patterns of SnO_2-based nanocrystalline materials towards CO. Sensor temperature: 200 (*a*), 250 (*b*), 300 (*c*) and 350 °C (*d*).[24]
CO content in air is 40 ppm; relative humidity is 30%.

Enhancement of the sensor response with increase in the operating temperature for other materials based on the modified SnO_2 suggests that adsorbed CO molecules are oxidized at the surface of the SnO_2 matrix by both bridging ions O^{2-} occupying terminal positions in the crystal lattice and by the adsorbed electrophilic oxygen species. Abrupt increase in the sensor response at an operating temperature of 300 °C correlates with the increase in the proportion of electrophilic atomic species $O^-_{(ads)}$ among the adsorbed oxygen species on the oxide surface. The atomic species react much more readily with the adsorbed carbon monoxide molecules. Since the sensor signal increases at the temperature much lower than that required to overcome the activation barrier to oxidation following the Mars–van Krevelen mechanism (~ 420 °C), participation of lattice oxygen in the oxidation of CO is of minor importance.[90]

In this connection, catalytic gold clusters present in the materials characterized by the highest sensor response towards CO can play a dual role. On the one hand, IR spectroscopy data[107] show that $O^-_{2(ads)}$ interacts with CO molecules on the surface of gold clusters; however, the intensity of corresponding absorption maxima in the IR spectra remains almost unchanged upon variation of the operating temperature that strongly influences transformations of CO on the surface. On the other hand, metallic gold clusters can additionally activate chemisorbed oxygen species in the vicinity of the three-phase boundary point $Au-SnO_2-gas$.[22] Despite the fact that these adsorbed oxygen species are not predominant on the surface, they are highly reactive and characterized by much shorter turnover time upon reaction with the reducing agent molecule. More exact data on this adsorbed oxygen species and on the mechanism of CO oxidation on the surface became available only recently in a study of the Au/TiO_2 system[108] which is to some extent similar to the system in question. The Au/TiO_2 system is widely used as low-temperature catalyst for the oxidation of volatile organic compounds.

4. Effect of surface acidity on the interaction with reducing gases

The acidity of the SnO_2 surface can be changed using modifiers the acidity of which is higher or lower than those of Sn^{2+} and Sn^{4+} cations on the surface of pure

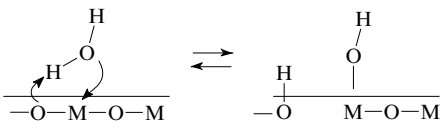
SnO_2. The choice of modifiers can be based on the concepts of oxide surface acidity (see above).

The content and strength of acid sites on the surface of oxides and other materials is measured using microcalorimetry methods and IR spectroscopy of probe molecules. Often, temperature-programmed desorption of ammonia (NH_3-TPD) is also used. The technique is suitable for measuring the strength and concentration of both Lewis and Brønsted acid sites.[109] The number of acid sites and their distribution with respect to the activation energy of ammonia desorption can be determined using a model[110] that assumes desorption of one ammonia molecule from each acid site.

Both pure and modified SnO_2 are characterized by the presence of two types of surface adsorption sites with different acidity. These are weak (desorption temperature from about 120 to 140 °C) and strong (desorption temperature is about 480 °C) acid sites (Fig. 13). Weak acid-base interaction of NH_3 with the surface materials corresponds to the Brønsted acid sites,[111] namely, hydroxyl groups that are present of the surface due to adsorption and dissociation of water molecules from air and due to the synthesis conditions. The NH_3 desorption peaks in the region ~110 °C (dashed line in Fig. 13) are clearly seen in the NH_3-TPD profiles of most materials under study. However, these peaks are absent in the TPD profiles of some materials that underwent high-temperature heat treatment during the synthesis and usually have a small specific surface area (SnO_2-500, SnO_2-700, Ru/SnO_2-700).[71] Strong adsorption sites are formed by the metal cations (Lewis acid sites) having incomplete oxygen environment on the surface of materials. These are Sn^{4+} with five oxygen atoms in the coordination sphere and Sn^{2+} with four oxygen atoms in the anionic environment. The binding energy of Sn^{2+} cations to NH_3 molecules is higher owing to an additional contribution of covalent interaction.[112] The peaks of NH_3 desorption from these acid sites are clearly seen in the NH_3-TPD profiles of the materials based on the pure SnO_2 and on SnO_2 modified with acidic modifiers (*e.g.*, V_2O_5, MoO_3).

Introduction of modifiers which optical basicity (Lewis acidity) differs from that of SnO_2 into the SnO_2 matrix is accompanied by changes in the total surface concentration of the acid sites;[41] this is first of all due to the changes in the number of weak acid sites, namely, surface hydroxyl groups (Fig. 14). Correspondence between the concentration of surface hydroxyl groups and the Lewis acidity of the material is ambiguous. However, one can assume that an increase in the charge of the metal cation facilitates dissociative adsorption of water molecules with the formation of two surface hydroxyl groups at the oxide surface.

Scheme 1



The introduction of modifiers with higher Lewis acidities into SnO_2 causes the number of surface hydroxyl groups to increase; this is accompanied by a decrease in the contribution of strong Lewis sites to the total acidity. It is to be emphasized that this behaviour was observed only for those materials based on nanocrystalline SnO_2 that were synthesized using the same procedure under identical heat treatment conditions, at 300 (see Fig. 14 *a*) and 500 °C (see Fig. 14 *b*).[71]

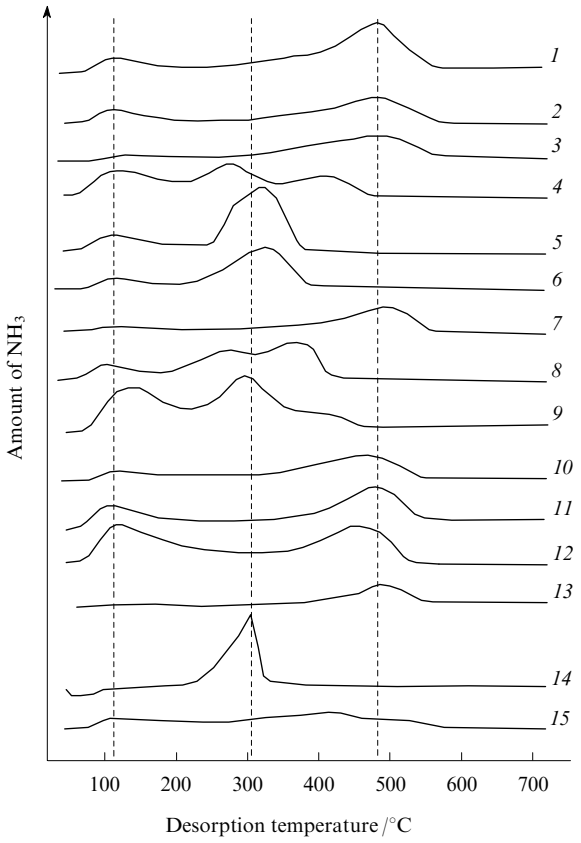


Figure 13. NH_3-TPD profiles for pure and chemically modified nanocrystalline SnO_2.[98]
Material: SnO_2 (*1*), Ni–Au/SnO_2 (*2*), Au/SnO_2 (*3*), Cr_2O_3/SnO_2 (*4*), Pd/SnO_2 (*5*), Ru/SnO_2 (*6*), SnO_2 (*7*), Pt/SnO_2 (*8*), Cr_2O_3/SnO_2 (*9*), Fe_2O_3/SnO_2 (*10*), MoO_3/SnO_2 (*11*), V_2O_5/SnO_2 (*12*), SnO_2 (*13*), Ru/SnO_2 (*14*) and La_2O_3/SnO_2 (*15*). Synthesis at: 300 (*1–6*); 500 (*7–12*) and 700 °C (*13–15*).

Studies of SnO_2 modified with Cr_2O_3, PdO_x, RuO_x and PtO_x revealed that peaks of ammonia desorption from the Lewis sites are shifted from 480 to 300 °C. Taking into account (i) rather high catalytic activity of deposited noble-metal clusters in many oxidation reactions and (ii) ready formation of chromyl anion Cr=O on the surface of nanocrystalline SnO_2 modified with Cr_2O_3,[113] the peaks at 300 °C can be attributed to desorption of products of partial dissociation of NH_3 followed by its oxidation on the surface rather than to desorption of NH_3.

5. Sensing properties of modified tin dioxide towards basic gases taking NH_3 as an example

According to the approach in question, an increase in the strength and concentration of the acid sites on the SnO_2 surface should lead to stronger sorption interaction of NH_3 with the sensor material. It is believed that at $T < 600$ °C, the major contribution to the sensor response comes from

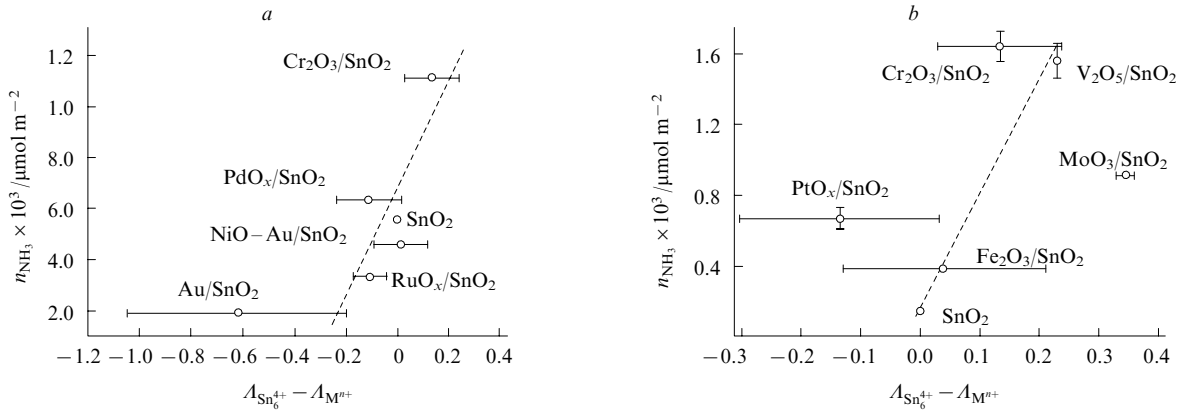


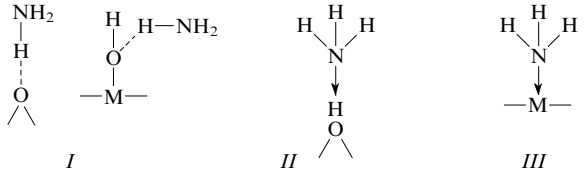
Figure 14. Correlations between concentrations of acid sites (n_{NH3}) on the surface of pure and modified SnO_2 and the optical basicity (Λ) difference between the Sn^{4+} cation in the octahedral oxygen environment and the modifier cation M^{n+} (see Ref. 71).
For the modifier cations, we used the average values of Λ and the intervals of their changes depending on the oxidation state of the coordination environment. Heat treatment temperature was 300 (*a*) and 500 °C (*b*).
Dashed lines denote the correlations.

the oxidation of NH_3 by oxygen chemisorbed on the surface of nanocrystalline SnO_2.[114]

$$2\beta NH_{3(gas)} + 3O^{-\alpha}_{\beta(ads)} \longrightarrow \beta N_{2(gas)} + 3\beta H_2O_{(gas)} + 3\alpha e^- \quad (29)$$

where $NH_{3(gas)}$ is the ammonia molecule in the gas phase and $N_{2(gas)}$, $H_2O_{(gas)}$ are the reaction product molecules desorbed from the surface of the sensor material to the gas phase.

Possible types of ammonia coordination on the oxide surface are as follows:



An ammonia molecule can be adsorbed with the formation of a hydrogen bond with the surface oxygen atom or with the oxygen atom of hydroxyl group (type *I*), a hydrogen bond between the nitrogen atom and the hydrogen atom of hydroxyl group (type *II*) or a donor-acceptor bond with the coordinatively unsaturated surface metal cation (type *III*).[103]

The formation of NH_4^+ ion on the SnO_2 surface is possible in the presence of surface Brønsted acid sites, whereas coordination of NH_3 molecules indicates the presence of Lewis acid sites. Dissociative adsorption of ammonia from the gas phase leads to formation of NH_2 and OH on the surface (Scheme 2).[103]

Scheme 2



Enhancement of the adsorption of NH_3 on the SnO_2 surface and, therefore, a stronger sensor signal can be achieved by increasing the number of the acid adsorption sites upon modification of the surface with cations characterized by stronger Lewis acidity than that of Sn^{4+} (*e.g.*, Mo^{6+}, V^{5+}). Indeed, such materials produce stronger sensor signals compared to pure SnO_2 or to materials modified with basic additives (*e.g.*, Fe_2O_3) at low operating temperatures (Fig. 15).[21, 71, 98] However, this advantage in the sensor signal magnitude over unmodified SnO_2 is insignificant, probably due to the competition between water and NH_3 molecules for the surface adsorption sites.

As in the case of CO, a pronounced increase in the SnO_2 sensor signal towards ammonia is observed upon modification of the matrix with catalytic gold clusters (Fig. 16). Weakening of the sensor signal observed at operating temperatures >250 °C for all sensor materials considered here is most probably due to a decrease in the degree of adsorption of ammonia[115] that is necessary for the sensing process to occur.

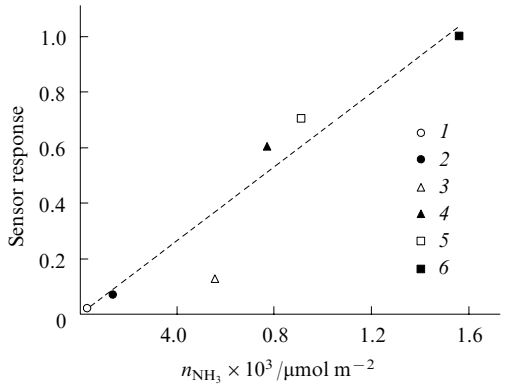


Figure 15. Sensor response to ammonia plotted *vs.* concentration of weak Brønsted acid sites (n_{NH_3}) on the surface of nanocrystalline materials based on SnO_2.[71]
Ammonia concentration in air is 20 ppm, the relative humidity is 30% and the sensor operating temperature is 200 °C.
Material: La_2O_3/SnO_2 (*1*), SnO_2 (*2*, *3*), Fe_2O_3/SnO_2 (*4*), MoO_3/SnO_2 (*5*) and V_2O_5/SnO_2 (*6*). Heat treatment temperature /°C: 700 (*1*, *2*), 300 (*3*) and 500 (*4*–*6*).

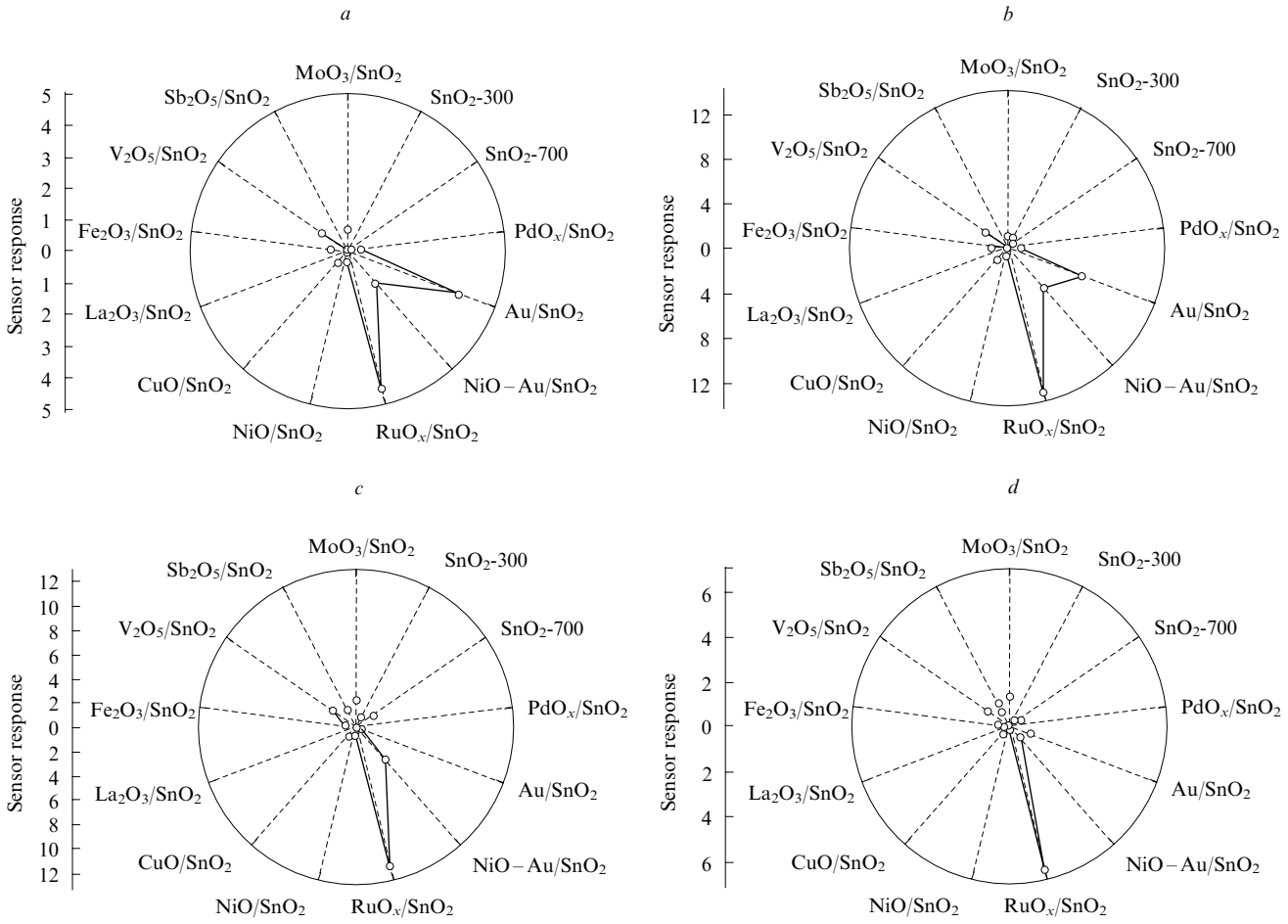


Figure 16. Sensitivity patterns of nanocrystalline materials based on SnO_2 towards NH_3 at sensor operating temperatures of 200 (*a*), 250 (*b*), 300 (*c*) and 350 °C (*d*).[24]
Ammonia concentration in air is 20 ppm and the relative humidity is 30%.

The strongest sensor response towards NH_3 is observed for Ru-modified SnO_2. The specific activity of RuO_2 as catalyst for the oxidation of NH_3 was discussed in the studies on the RuO_2/TiO_2 system.[116, 117] It was shown that dissociation of NH_3 molecules followed by oxidation occurs in the temperature range from 300 to 400 °C; as a result, NO_3^- groups are adsorbed on the surface of titania particles and NO^- groups are adsorbed on the surface of ruthenia particles. In addition, some contribution comes from the surface of metallic ruthenium that activates dissociation of molecularly adsorbed ammonia.[118] Most intense dissociation occurs on stepped surfaces and is accompanied by the formation of atomic nitrogen that is tightly bound to the surface,

$$NH_{3(gas)} + Ru(0001) \underset{k_{des}}{\overset{k_{ads}}{\rightleftarrows}} NH^{+*}_{3(ads)} \ldots \quad (30)$$

$$NH^{+*}_{3(ads)} \ldots \underset{k_{destr}}{\overset{k_{dif}}{\rightleftarrows}} NH^{-*}_3 \quad (31)$$

$$NH^{-*}_3 \xrightarrow{k_{dis}} N^{-}* + 3\,H_{(ads)} \quad (32)$$

$$N^{-}* + 3\,H_{(ads)} \xrightarrow{k_{N(dif)}} N_{(ads)} + 3\,H_{(ads)} \quad (33)$$

where $NH_{3(gas)}$ is the ammonia molecule in the gas phase; Ru(0001) is the metallic ruthenium surface; k_{ads} and k_{des} are the adsorption and desorption constants, respectively; $NH_{3(ads)}$ is the ammonia molecule adsorbed on the metal surface (the active site of NH_3 dissociation is asterisked); k_{dif} is the diffusion constant of adsorbed NH_3 molecule, k_{destr} is the decomposition constant of the complex between the adsorbed ammonia molecule and the active site, NH_3^{-*} is the ammonia molecule adsorbed on the dissociation site on the surface of metallic ruthenium, k_{dis} is the dissociation constant, $N^{-}*$ is the nitrogen atom adsorbed on the dissociation site on the surface of metallic ruthenium, $k_{N(dif)}$ is the constant of diffusion of atomic nitrogen across the ruthenium surface, $N_{(ads)}$ is the nitrogen atom that left the dissociation site and $H_{(ads)}$ is the adsorbed hydrogen atom.

Interaction between the adsorbed species O^- and atomic nitrogen

$$N_{(ads)} + O^-_{(ads)} \longrightarrow NO_{(ads)} + e^- \quad (34)$$

resulting in highly reactive nitrosyl radical species NO can additionally influence chemical transformations on the sur-

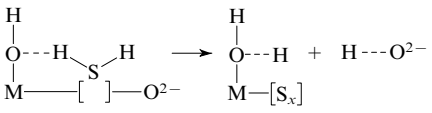
face. These species can play the role of additional adsorption sites and be centres of chemical transformations of NH_3 molecules accompanied by abrupt increase in the sensor response.[118, 119]

6. Sensing properties of modified tin dioxide towards acidic gases taking H_2S as an example

Interaction of gaseous hydrogen sulfide with oxide surfaces is governed by two factors. First, the compound is a rather strong reducing agent (ionization potential of H_2S molecule is 10.4 eV). Second, hydrogen sulfide is a Brønsted acid with the S–H bond capable of readily undergoing a heterolytic cleavage, especially in the formation of donor-acceptor bonds. The interaction with gaseous hydrogen sulfide on oxide surfaces leads to the following changes:[103]

— formation of sulfides (square brackets denote the surface oxygen vacancy)

$$M^{n+}—O^{2-} \xrightarrow{H_2S} M^{n+}—\left(S—H\right)^{-} + H^{+}—O^{2-} \qquad (35)$$



(36)

— partial blockage of the Lewis acid sites

$$M^{n+}—O^{2-} \xrightarrow{H_2S} —M—S^{2-} + H_2O \qquad (37)$$

— reduction of mixed-valence metal cations

$$M^{n+}O^{2-} + H_2S \longrightarrow [S_x] + M^{(n-2)+} + H_2O \qquad (38)$$

— oxidation of sulfur and enhancement of the surface acidity owing to formation of SO_x groups.

Thus, enhanced sensor response can be expected upon increasing the surface concentration of basic sites and reducing the surface acidity owing to doping the oxide matrix with cations having higher basicities than Sn^{2+} or Sn^{4+}.

An analysis of experimental data (Fig. 17) showed that the sensor signals of SnO_2-based materials towards hydrogen sulfide pass through minima as the operating temperature increases. The maximum sensitivity observed at 200 °C is most probably due to H_2S adsorption that decreases as temperature increases. Enhancement of the sensor response with increasing the operating temperature >300 °C is probably due to activation of the formation of atomic chemisorbed oxygen species that are involved in the oxidation of adsorbed H_2S on the surface

$$\beta H_2S_{(gas)} + 3\,O^{-\alpha}_{\beta(ads)} \longrightarrow \beta SO_{2(gas)} + \beta H_2O_{(gas)} + 3\alpha e^{-} \qquad (39)$$

In this connection, enhancement of the sensor sensitivity of materials based on nanocrystalline SnO_2 upon modification of the surface with catalytic gold clusters deserves attention;[24] this is consistent with the data obtained in experiments with other reducing gases.

Changes in the surface acidity of nanocrystalline SnO_2 have no distinct influence on the sensor response. The maximum enhancement of the sensor signal was observed upon modification of SnO_2 of with copper and iron oxides. We believe an abrupt increase in the sensor response is not associated with changes in the surface acidity. The phenomenon can be explained taking into account the chemical nature of the modifiers that show high sulfur affinity and readily form sulfides in the course of heterolytic reaction of H_2S molecule with the acid–base Lewis pair on the oxide surface (a chemical transformation of highly resistive p-type semiconductor CuO ($\rho = 10^5$ Ω cm) and n-type semiconductor Fe_2O_3 ($\rho = 10^{10}–10^{13}$ Ω cm) to highly conductive sulfides Cu_2S and FeS).[20] For instance,

$$6\,CuO + 4\,H_2S_{(gas)} \longrightarrow 3\,Cu_2S + SO_{2(gas)} + 4\,H_2O_{(gas)} \qquad (40)$$

An abrupt change in the conductivity is due to removal of energy barriers between SnO_2 grains and the oxide modifier grains, being followed by a rapid increase in the conductivity of the material. Raising the temperature causes the sensor signal to decrease owing to fast oxidation of sulfides to oxides.

The data presented here point to correctness of the concepts used to synthesize heterogeneous catalysts with specified surface acidity and catalysts for heterogeneous oxidation to be utilized in gas sensors. It should be noted that the changes in the strength and concentration of acid sites on the surface of nanocrystalline SnO_2 make insignificant contribution to the sensor response towards reducing gases; this emphasizes that the redox processes contribute to a larger extent than the sorption processes (see above).

7. Sensing properties of modified tin dioxide towards volatile organic compounds taking acetone and ethanol as examples

A huge class of reducing agents includes volatile organic compounds with various chemical structures. Acetone can be treated as a Lewis base because its molecule contains a carbonyl group; also, one can expect that enhancement of the surface acidity of modified nanocrystalline SnO_2 will lead to higher sensor sensitivity. On the contrary, ethanol can be considered as an acid owing to weak Brønsted acidity exhibited by alcohols.

The temperature dependence of the sensor response towards acetone vapours from materials based on modified SnO_2 (Fig. 18) resembles the temperature dependence of the sensor response to CO (see Fig. 12). Therefore, it is reasonable to assume that the oxidation of organic component adsorbed on the surface by chemisorbed oxygen will also make the major contribution to the increase in the sensor signal with increasing the operating temperature.[24] However, no low-temperature sensor response characteristic of Pd-modified materials used for CO detection is observed in this case. Disappearance of this signal cannot be associated with insufficiently high reactivity of the atomic oxygen species adsorbed on the surface of PdO_x clusters and playing the key role in the oxidation of CO because the acetone molecule is much more reactive than CO.

The lack of the low-temperature sensor response towards acetone vapours in the case of PdO_x/SnO_2 can be

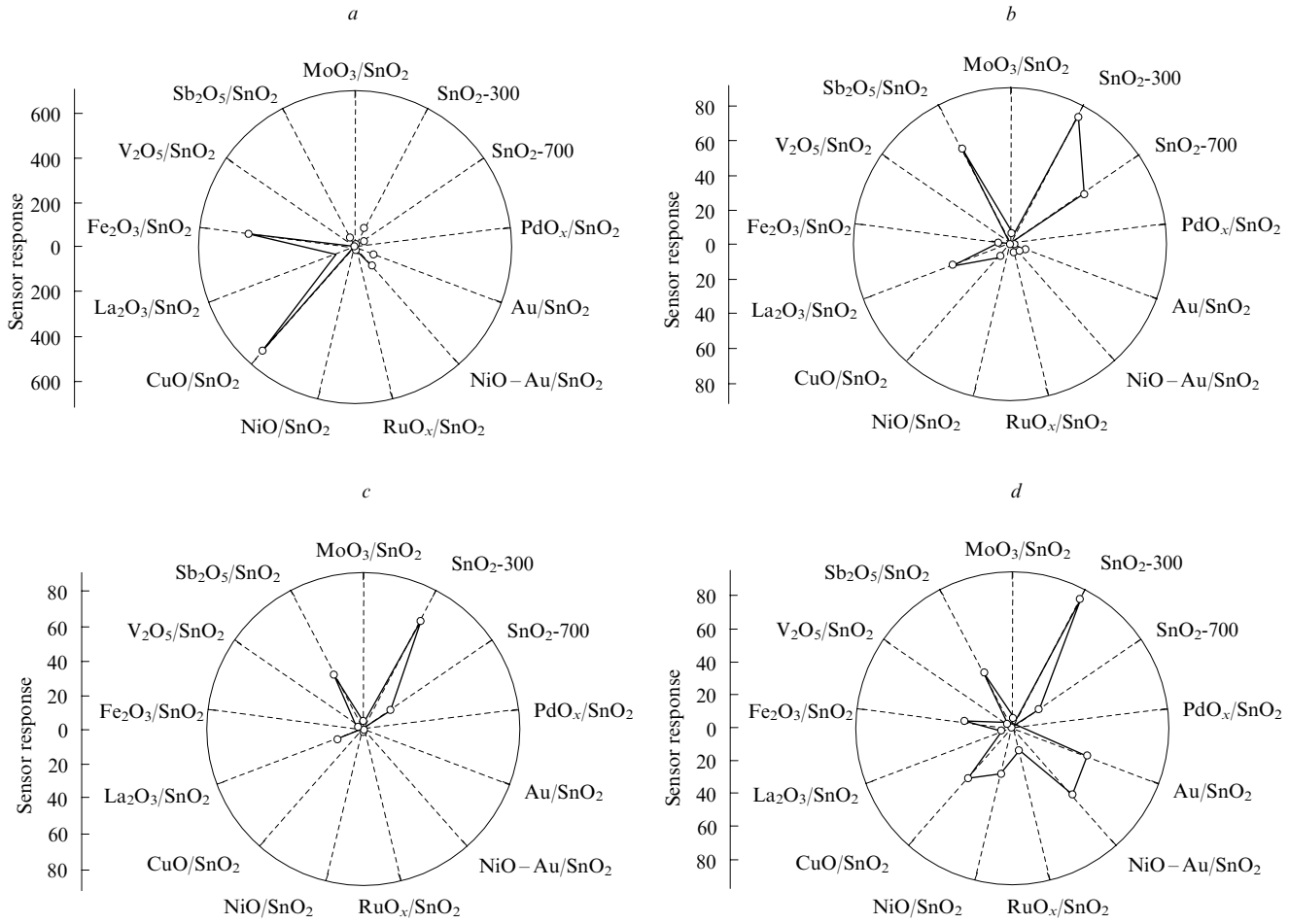


Figure 17. Sensitivity patterns of nanocrystalline materials based on SnO_2 towards H_2S at sensor operating temperatures of 200 (*a*), 250 (*b*), 300 (*c*) and 350 °C (*d*).[24]
H_2S concentration in air is 2 ppm and the relative humidity is 30%.

explained by blockage of reverse spillover of oxygen species due to the reduction of the concentration of the chemisorbed oxygen species on the surface of the oxide matrix. These species can be involved in partial oxidation of adsorbed acetone molecules on the SnO_2 surface, the newly formed oxidation products at low temperatures being not desorbed from the surface; as a consequence, active sites of formation of electrophilic adsorbed oxygen species on the surface are not recovered. This limitation is removed upon an increase in the sensor operating temperature, as is clearly demonstrated by Ru-modified SnO_2. As in the case of CO detection, a local maximum of the sensitivity to acetone vapours is observed at 300 °C.

Materials modified with gold clusters also demonstrate a maximum sensor response towards acetone, but only at 350 °C. Lowering the temperature to 300 °C causes an abrupt decrease in the sensor response. This may indicate that the oxidation of acetone on the surface of an oxide matrix is a more complicated surface process compared to the oxidation of CO and simultaneously follows several channels resulting in the formation of some intermediates. According to published data,[120] incomplete oxidation of acetone on the oxide surface may result in various organic compounds including saturated hydrocarbons, carboxylic acids as well as aldol condensation products,[121] *e.g.*, acrolein, 2,4-dimethylfuran or pent-3-en-2-one.

Thus, the sensor response of materials based on nanocrystalline SnO_2 towards acetone and other volatile organic compounds can be governed by the rate and completeness of recovery of the initial conductivity of sensor materials in pure air atmosphere rather than by an increase in conductivity in the course of interaction with these compounds. Recovery may require (i) desorption of products of incomplete oxidation and subsequent full oxidation of these products to CO_2 or (ii) prevention of reactions resulting in oxygen-containing compounds with higher molecular mass compared to acetone. That is why the high sensor response is only observed at elevated operating temperatures where the interaction with the gas phase ensures predominance of complete oxidation of acetone molecules adsorbed on the surface to CO_2 and H_2O (see Ref. 122)

$$Me_2CO_{(gas)} + \frac{8}{\beta} O^{-\alpha}_{\beta(ads)} \longrightarrow 3\,CO_{2(gas)} + 3\,H_2O_{(gas)} + \frac{8\alpha}{\beta} e^- \quad (41)$$

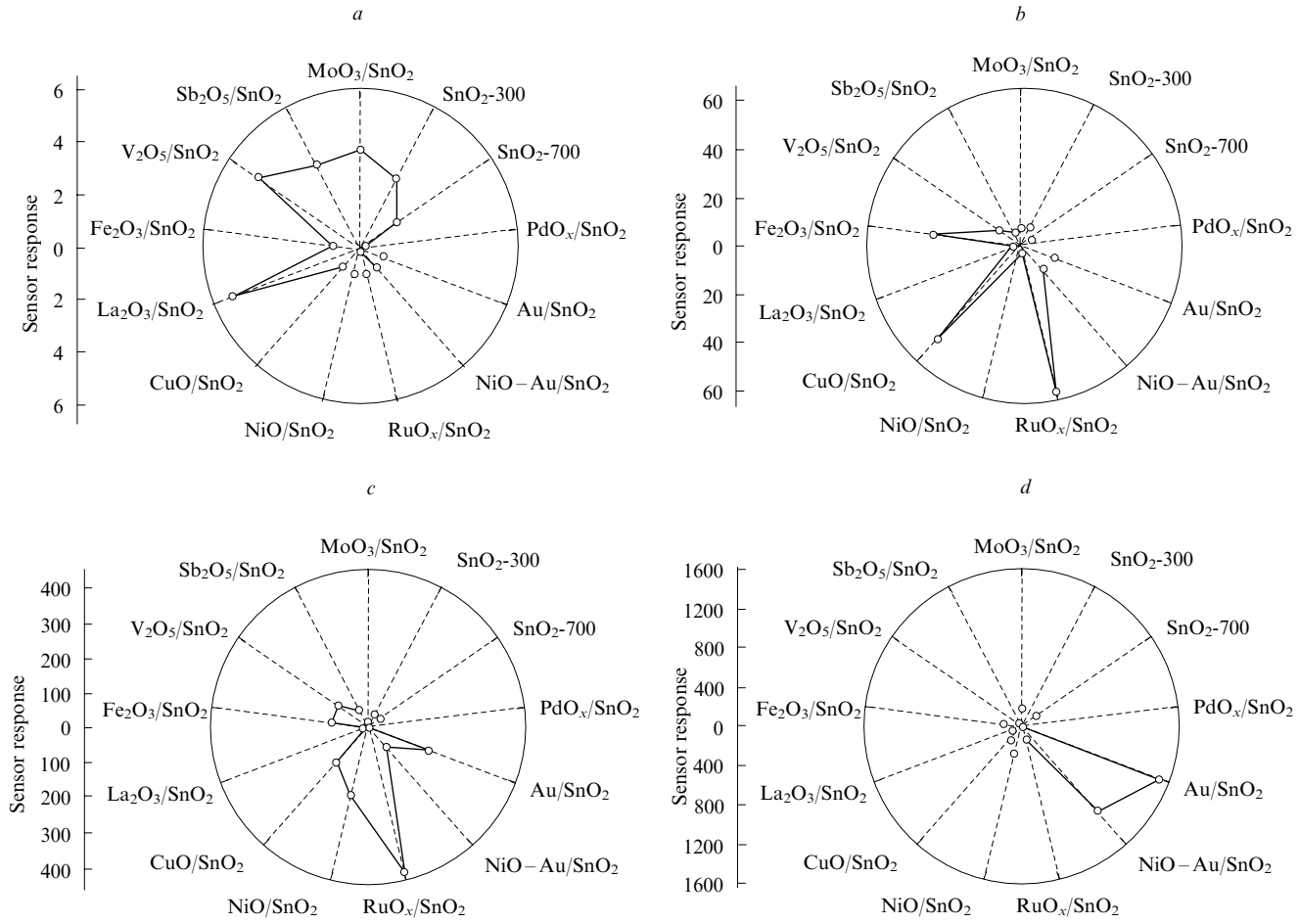


Figure 18. Sensitivity patterns of SnO_2-based nanocrystalline materials towards acetone vapours. Sensor operating temperature: 200 (*a*), 250 (*b*), 300 (*c*) and 350 °C (*d*).[24] Concentration of acetone vapours in air is 130 ppm and the relative humidity is 30%.

It is just incomplete oxidation of acetone on the oxide surface than can be influenced by the modification of SnO_2 with oxide clusters the acidity of which is higher or lower than that of SnO_2. Different combinations of products of incomplete oxidation may facilitate or, *vice versa*, hamper recovery of the surface initial state after the sensor interaction which in turn may strongly influence the sensor response. In the course of adsorption on the oxide surface, acetone undergoes a tautomeric rearrangement resulting in the enol form,[120] which, unlike the keto form, is adsorbed on the basic sites that can be of greater importance for the activation of sorption interaction with acetone vapours than the acid sites. However, this effect was not experimentally observed so far and the number of studies on this approach to modification of the sensing properties of SnO_2 is too small to generalize the available information. At the same time, a clearly seen dependence of the sensor sensitivity on the surface acidity is observed in the detection of ethanol vapours.[98, 123]

There are two main chemical paths of ethanol conversion in the course of a heterogeneous reaction with the surface of oxide materials, *viz*., dehydration resulting in ethylene and oxidative dehydrogenation affording acetaldehyde.[123] Oxidative dehydrogenation involves [124]

— dissociative adsorption;

— oxidative elimination of hydrogen atom from C_α atom;

— desorption of water; and

— re-oxidation of the catalyst surface by atmospheric air.

This type of interaction is accompanied by changes in the conductivity owing to the reaction with chemisorbed oxygen

$$\beta\,\mathrm{EtOH} + \mathrm{O}^{-\alpha}_{\beta(\mathrm{ads})} \longrightarrow \beta\,\mathrm{MeCHO} + \beta\,\mathrm{H_2O} + \alpha\,\mathrm{e}^- \qquad (42)$$

If samples have equal specific surface areas, the selectivity of ethanol conversion to acetaldehyde depends on the concentration ratio of the strong (Lewis) and weak (Brønsted) acid sites.

If the surface is mainly covered with the Brønsted sites, dehydration of ethanol to C_2H_4 occurs:

$$\mathrm{EtOH} \longrightarrow \mathrm{C_2H_4} + \mathrm{H_2O} \qquad (43)$$

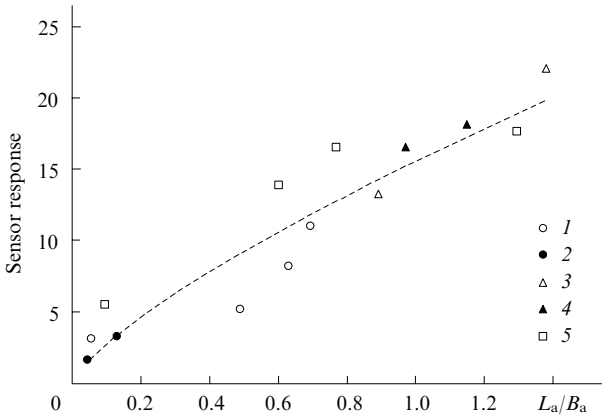


Figure 19. Sensor response towards ethanol vapours plotted *vs.* the concentration ratio of the Lewis (L_a) and Brønsted (B_a) acid sites on the surface of sensor materials.
Concentration of ethanol vapours in air is 10 ppm and the relative humidity is 2%.
Material: MoO_3/SnO_2 (*1*), V_2O_5/SnO_2 (*2*), In_2O_3/SnO_2 (*3*), La_2O_3/SnO_2 (*4*) and Fe_2O_3/SnO_2 (*5*).

The process is not accompanied by changes in the concentration of charge carriers; therefore, a low electrical response is expected for materials with high proportion of the surface Brønsted acid sites in the presence of ethanol vapours. On the contrary, an increase in the proportion of the Lewis acid sites should favour enhancement of the sensor response. Also, an increase in the conductivity of n-type semiconductor oxides in the presence of ethanol vapours can also be due to oxidation of the intermediates MeCHO and C_2H_4 to CO_2 and H_2O

$$\beta\,MeCHO_{(gas)} + 5\,O^{-\alpha}_{\beta(ads)} \longrightarrow \longrightarrow 2\beta\,CO_{2(gas)} + 2\beta\,H_2O_{(gas)} + 5\alpha\,e^- \quad (44)$$

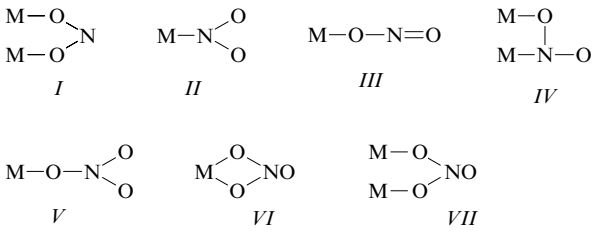
$$\beta\,C_2H_{4(gas)} + 6\,O^{-\alpha}_{\beta(ads)} \longrightarrow \longrightarrow 2\beta\,CO_{2(gas)} + 2\beta\,H_2O_{(gas)} + 6\alpha\,e^- \quad (45)$$

For nanocomposites based on nanocrystalline SnO_2, the sensor response towards ethanol correlates with the ratio of the surface concentrations of the Lewis and Brønsted acid sites (Fig. 19).[23, 40, 97]

8. Sensing properties of modified tin dioxide towards oxidizing gases taking NO_2 as an example

Oxidizing gases are not so abundant as reducing gases and first of all include NO_2, ozone, chlorine and sulfur dioxide. The sensor response towards oxidizing gases is due to electron density transfer from the conduction band of SnO_2 to the adsorbed gas molecule, accompanied by an increase in the resistance of the sensing layer.[10, 119] Thus, one can assume that high selectivity towards reducing gases in the detection of oxidizing gases can be attained by creating conditions for easy transfer of electron density to adsorbed molecules.

Interaction of NO_2 molecules with the oxide surfaces can proceed by the molecular and dissociative adsorption mechanisms. The corresponding models are shown below.



Molecular adsorption may involve the formation of various nitrite (NO_2) and nitrate (NO_3) surface groups.[103]

Numerous published data indicate that the interaction between n-type semiconductor oxides and NO_2 is accompanied by a decrease in conductivity, *i.e.*, nitrogen dioxide, like oxygen, is an electron density acceptor. Therefore, the interaction of NO_2 with the Lewis acidic surface sites resulting in nitronium ion (see model *II*)

$$NO_2 + M^{n+} \longrightarrow NO_2^+ + M^{(n-1)+} \quad (46)$$

is not responsible for the change in the conductivity of materials.

The electron affinity energy of NO_2 molecule much exceeds that of oxygen molecule [2.27 eV (Ref. 125) *vs.* 0.44 eV (Ref. 126), respectively]. This governs the possibility of detecting low NO_2 concentrations in air (<1 ppm) in the presence of $\sim$20 vol.% of oxygen. A Raman spectroscopy study[127] revealed that in the presence of NO_2, the conductivity of SnO_2 correlates with the concentration of the bidentate surface nitrite groups. The results of *ab initio* calculations[128] suggest that adsorption of NO_2 molecule with coordination of one or both oxygen atoms to the bridging oxygen vacancies of partially reduced SnO_2 surface is the most energetically favourable process (see models *I*, *III*, *VI* and *VII*).

An IR spectroscopic and TPD study[129] in the temperature range 25–400 °C revealed the possibility of NO_2 dissociation in the interaction with the SnO_2 surface. The presence of NO molecules among TPD products can be indirect evidence of the occurrence of the following reactions:

$$NO_{2(gas)} \longrightarrow NO_{2(ads)} \quad (47)$$

$$NO_{2(ads)} + e^- \longrightarrow NO^-_{2(ads)} \quad (48)$$

$$NO^-_{2(ads)} \longrightarrow NO_{(gas)} + O^-_{(ads)} \quad (49)$$

As the measuring temperature increases, the sensor response of both pure and modified SnO_2 towards NO_2 decreases (Fig. 20). A high sensor signal was observed for MoO_3-modified SnO_2; this can be due to the ability of Mo atoms to exist in the mixed oxidation state and be present in the crystal structure of the near-surface layers of SnO_2 grains in the Mo^{5+} form[130, 131]

$$Mo_{Sn}^{6+} + V_O^{\bullet} \longrightarrow Mo_{Sn}^{5+} + V_O^{\bullet\bullet} \quad (50)$$

or

$$Mo_i^{6+} + e \longrightarrow Mo_i^{5+} \quad (51)$$

(here we use the Kröger–Vink notations of point defects in crystals, namely, $V_O^{\bullet}$ and $V_O^{\bullet\bullet}$ are the oxygen vacancies bearing a single and double positive charge, respectively; the subscript 'Sn' denotes the cation occupying a tin lattice site in the crystal structure of the oxide; and the subscript '*i*' denotes the cation occupying an interstitial site).

The Mo^{5+} cation occupying the lattice site in the structure of the oxide matrix can be oxidized again with ease to Mo^{6+}. Therefore, in the case of adsorption of NO_2 molecules on the SnO_2 surface, Mo atoms can act as receptors. Transfer of electron density from the Mo atoms to the chemisorbed species NO_x^- abruptly decreases the conductivity of the oxide material.

High sensor responses of NiO-modified materials towards NO_2 can be explained by analogy by the effect of the oxidation of the modifier. According to a classification,[73] NiO is a readily oxidizable oxide. Adsorption of molecules characterized by high electronegativities is accompanied by the following transformation in the near-surface layers:

$$Ni^{2+} \longrightarrow Ni^{3+}$$

Thus, nitrogen dioxide having much higher electron affinity energy than oxygen (see above) can promote the oxidation of Ni^{2+} on the surface of the NiO-modified material, which affects the magnitude of the sensor signal.

Incorporation of Sb^{5+} cations into nanocrystalline SnO_2 leads to a similar effect. This procedure is a well-known method of increasing the concentration of charge carriers in the near-surface layer of nanocrystalline SnO_2 grains.[132, 133] Since nitrogen dioxide exhibits pronounced

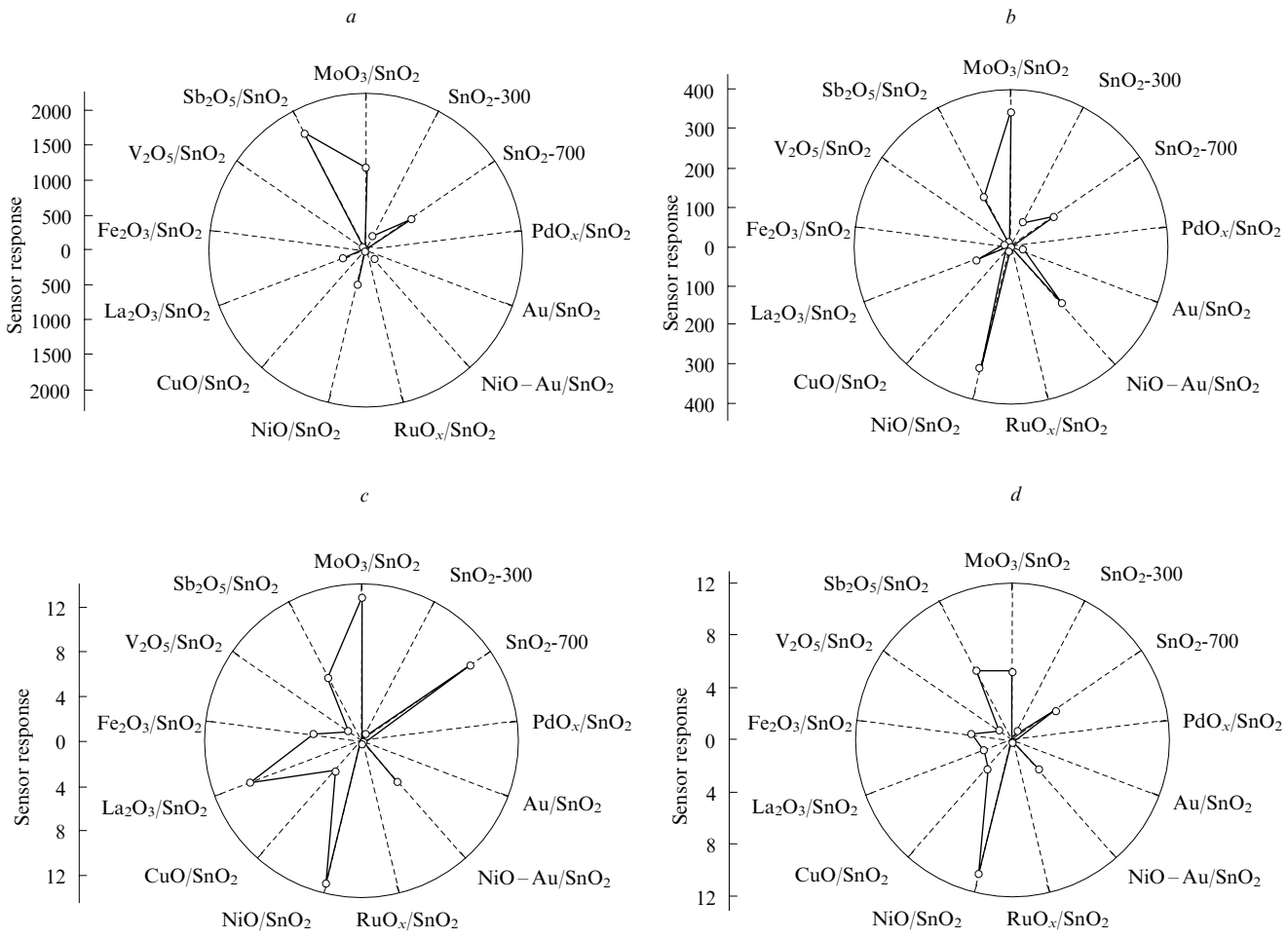


Figure 20. Sensitivity patterns of SnO_2-based nanocrystalline materials towards NO_2 at sensor operating temperatures of 200 (*a*), 250 (*b*), 300 (*c*) and 350 °C (*d*).[24]
NO_2 content in air is 3 ppm and the relative humidity is 30%.

properties of electron density acceptor, an increase in the concentration of electrons with energies that are high enough to overcome the barrier produced by the negatively charged surface favours the occurrence of reaction (48), which is responsible for the formation of the sensor signal.

Note that this interpretation of physicochemical processes accompanying the detection of NO_2 using metal-oxide semiconductors is simplified and requires some revision. It should be emphasized that the contribution of the modifier-induced change in the reactivity of the surface of sensor materials to the formation of the sensor signal is a minor factor. Its observation in the case of, *e.g.*, chemically modified nanocrystalline SnO_2 is precluded by large electrophysical effects underlying the sensor responses.

From the utilitarian point of view, it is important that doping the oxide matrix with cations capable of going to higher oxidation states in the course of modification procedure or during the adsorption of gas molecules ensures high sensing properties of the surface of modified nanocrystalline SnO_2 towards oxidizing gases. A comparison of the sensor sensitivity patterns revealed low sensitivity of these materials (*e.g.*, MoO_3/SnO_2) towards reducing gases; therefore, oxidizing gases can be detected with high selectivity.

IV. Conclusion

In this review, we demonstrated the applicability of the theoretical concepts relating the chemical structure to the reactivity of the surfaces of solids in the interaction with gases, for directed variation of the acidity and sorption properties of the surface of nanocrystalline SnO_2. Moreover, we demonstrated a proportional effect of the concentration of acid sites on the sensor response of materials towards a basic gas (NH_3).

We have considered a number of mechanisms of the redox interaction between materials based on nanocrystalline SnO_2 and reducing gases, which leads to formation of a pronounced sensor response. In accordance with these mechanisms, the major contribution to the solid–gas chemical interaction comes from the chemisorbed oxygen species; the contribution of mobile lattice oxygen species in the near-surface layers of nanocrystalline grains and, as a consequence, changes in the conductivity are of minor importance. The activity of sensor interaction correlates with the predominant type and concentration of chemisorbed oxygen species on the surface of SnO_2 grains.

Most gases to be detected belong to reducing gases. Also, there is a variety of mechanisms of the sorption and redox interaction of gases with the surface of oxide materials. Because of this, the regularities considered in this review taking simple gases as examples cannot be directly used in the design of novel composite metal-oxide sensor materials. The development of methods for directed synthesis of sensor materials with high selectivity and sensitivity towards more complex gases and vapours of organic compounds requires new experimental data including those obtained from *in operando* and *in situ* experiments.

This review has been written under financial support from the Russian Foundation for Basic Research (Project No. 12-03-31446).

References

1. I A Myasnikov, V Ya Sukharev, L Yu Kupriyanov, S A Zav'yalov *Poluprovodnikovye Sensory v Fiziko-Khimicheskikh Issledovaniyakh* (Semiconductor Sensors in Physicochemical Investigations) (Moscow: Nauka, 1991)
2. B F Myasoedov, A V Davydov *Zh Anal. Khim.* **45** 1259 (1990) [a]
3. T C Pearce, S S Schiffman, H T Nagle, J W Gardner *Handbook of Machine Olfaction: Electronic Nose Technology* (Weinheim: Wiley-VCH, 2003)
4. G Korotcenkov, B K Cho *Prog. Cryst. Growth Charact. Mater.* **58** 167 (2012)
5. D E Williams, in *Solid State Gas Sensors* (Eds P T Mosely, B C Tofield) (Bristol: Alam Higer, 1987)
6. W Göpel, K D Schierbaum *Sens. Actuators, B* **26** 1 (1995)
7. E Souteyrand *Transduction Electrique pour la Detection de Gaz. Les Capteurs Chimiques* (Lyon: CMC2, 1997) p. 15
8. F F Vol'kenshtein *Elektronnye Protsessy na Poverkhnosti Poluprovodnikov* (Electronic Processes on Semiconductor Surface) (Moscow: Nauka, 1987)
9. S Morrison *Chemical Physics of Surfaces* (New York: Plenum, 1977)
10. N Bârsan, U Weimar *J. Electroceram.* **7** 143 (2001)
11. P Althainza, A Dahlke, J Goschnick, H J Ache *Thin Solid Films* **241** 344 (1994)
12. A Ryzhikov, M Labeau, A Gaskov *Sens. Actuators, B* **109** 91 (2005)
13. X Huang, L Wang, Y Sun, F Meng, J Liu *Sens. Actuators, B* **99** 330 (2004)
14. J O W Norris, in *Solid State Gas Sensors* (Eds P T Mosely, B C Tofield) (Bristol: Alam Higer, 1987) p. 124
15. D Kohl *Sens. Actuators, B* **1** 158 (1990)
16. N Yamazoe, Y Kurokawa, T Seyama *Sens. Actuators* **4** 283 (1983)
17. N Yamazoe *Sens. Actuators, B* **5** 7 (1991)
18. J F McAleer, P T Moseley, J O W Norris, D E Williams, B C Tofield *J. Chem. Soc., Faraday Trans. 1* **84** 441 (1988)
19. J Mizsei *Sens. Actuators, B* **23** 173 (1995)
20. M N Rumyantseva, O V Safonova, M N Bulova, L I Ryabova, A M Gaskov *Russ. Chem. Bull., Int. Ed.* **52** 1151 (2003)
21. M N Rumyantseva, A M Gaskov *Russ. Chem. Bull., Int. Ed.* **57** 1086 (2008)
22. P Montmeat, J-C Marchand, R Lalauze, J-P Viricelle, G Tournier, C Pijolat *Sens. Actuators, B* **95** 83 (2003)
23. J Arbiol, J R Morante, P Bouvier, T Pagnier, E Makeeva, M Rumyantseva, A Gaskov *Sens. Actuators, B* **118** 156 (2006)
24. V Krivetskiy, A Ponzoni, E Comini, S Badalyan, M Rumyantseva, A Gaskov *Electroanalysis* **22** 2809 (2010)
25. I Matko, M Gaidi, J L Hazemann, B Chenevier, M Labeau *Sens. Actuators, B* **59** 210 (1999)
26. A Marikutsa, V Krivetskiy, L Yashina, M Rumyantseva, E Konstantinova, A Ponzoni, E Comini, A Abakumov, A Gaskov *Sens. Actuators, B* **175** 186 (2012)
27. M Gaidi, J L Hazemann, I Matko, B Chenevier, M Rumyantseva, A Gaskov, M Labeau *J. Electrochem. Soc.* **147** 3131 (2000)
28. D Koziej, M Hübner, N Bársan, U Weimar, M Sikora, J-D Grunwaldt *Phys. Chem. Chem. Phys.* **11** 8620 (2009)
29. A V Marikutsa, M N Rumyantseva, A M Gaskov, E A Konstantinova, D A Grishina, D M Deygen *Thin Solid Films* **520** 904 (2011)

30. G Korotcenkov *Sens. Actuators, B* **107** 209 (2005)
31. N Bârsan, D Koziej, U Weimar *Sens. Actuators, B* **121** 18 (2007)
32. H Idriss, E G Seebauer *Catal. Lett.* **66** 139 (2000)
33. H Idriss, M Barteau *Adv. Catal.* **45** 261 (2000)
34. R Schlögl *CATTECH* **5** 146 (2001)
35. R K Grasselli *Top. Catal.* **21** 79 (2002)
36. A Gurlo, N Bârsan, U Weimar, in *Metal Oxides: Chemistry and Applications* (Ed. J L G Fierro) (Boca Ration, FL: CRC Press, Taylor and Francis, 2006) p. 683
37. M Calatayud, A Markovits, M Menetrey, B Mguig, C Minot *Catal. Today* **85** 125 (2003)
38. A Gervasini, G Bellussi, J Fenyvesi, A Auroux *J. Phys. Chem.* **99** 5117 (1995)
39. G Connell, J A Dumesic *J. Catal.* **105** 285 (1987)
40. L Daza, S Dassy, B Delmon *Sens. Actuators, B* **10** 99 (1993)
41. M Rumyantseva, V Kovalenko, A Gaskov, E Makshina, V Yuschenko, I Ivanova, A Ponzoni, G Faglia, E Comini *Sens. Actuators, B* **118** 208 (2006)
42. G Busca *Phys. Chem. Chem. Phys.* **1** 723 (1999)
43. D Barthomeuf *J. Phys. Chem.* **88** 42 (1984)
44. M Niwa, Y Habuta, K Okumura, N Katada *Catal. Today* **87** 213 (2003)
45. A Auroux, A Gervasini *J. Phys. Chem.* **94** 6371 (1990)
46. E Bordes-Richard *Top. Catal.* **50** 82 (2008)
47. J A Duffy, M D Ingram *J. Am. Chem. Soc.* **93** 6448 (1971)
48. Y Zhang *Inorg. Chem.* **21** 3886 (1982)
49. Y Zhang *Inorg. Chem.* **21** 3889 (1982)
50. C K Jorgensen *Absorption Spectra and Chemical Bonding in Complexes* (New York: Pergamon Press, 1962)
51. A L Tchougreeff, R Dronskowski *Int. J. Quant. Chem.* **109** 2606 (2009)
52. J A Duffy *Geochim. Cosmochim. Acta* **57** 3961 (1993)
53. A Lebouteller, P Courtine *J. Solid State Chem.* **137** 94 (1998)
54. P Moriceau, A Lebouteller, E Bodres, P Courtine *Phys. Chem. Chem. Phys.* **1** 5735 (1999)
55. J Portier, G Campet, J Etourneau, B Tanguy *J. Alloys Compd.* **209** 285 (1994)
56. J Portier, G Campet, J Etourneau, M C R Shastry, B Tanguy *J. Alloys Compd.* **209** 59 (1994)
57. E A Mamedov, V P Vislovskii, R M Talyshinskii, R G Rizayev *Stud. Surf. Sci. Catal.* **72** 379 (1992)
58. J A Duffy *J. Solid State Chem.* **62** 145 (1986)
59. J R Tessman, A H Kahn, W Shockley *Phys. Rev.* **92** 890 (1953)
60. J A Duffy *J. Phys. Chem.* **110** 13245 (2006)
61. E Iguchi, H Nakatsugawa *Phys. Rev. B* **51** 10956 (1995)
62. R T Sanderson *Science* **114** 670 (1951)
63. R T Sanderson *J. Am. Chem. Soc.* **97** 1367 (1975)
64. N C Jeong, J S Lee, E L Tae, Y J Lee, K B Yoon *Angew. Chem. Int. Ed.* **47** 10128 (2008)
65. A C C Rodrigues *J. Math. Chem.* **37** 347 (2005)
66. M Huang, A Adnot, S Kaliaguine *J. Am. Chem. Soc.* **114** 10005 (1992)
67. M Henry *Mater. Sci. Forum* **152–153** 355 (1994)
68. P Nortier, A P Borosy, M Allavena *J. Phys. Chem. B* **101** 1347 (1997)
69. J L L Murrel, L G Soled *J. Phys. Chem.* **91** 1526 (1987)
70. A Shiga, N Katada, M Niva *Catal. Today* **111** 333 (2006)
71. V Krivetskiy, M Rumyantseva, A Gaskov, in *Metal Oxide Nanomaterials for Chemical Sensors, Integrated Analytical Systems* (Eds M A Carpenter, S Mathur, A Kolmakov) (New York: Springer, 2013) p. 69
72. E Becker, P-A Carlsson, L Kylhammar, M A Newton, M Skoglundh *J. Phys. Chem. C* **115** 944 (2011)
73. A Bielański, J Haber *Catal. Rev.* **19** 1 (1979)
74. G Busca, E Finocchio, G Ramis, G Ricchiardi *Catal. Today* **32** 133 (1996)
75. P Mars, D W van Krevelen *Chem. Eng. Sci.* **3** 41 (1954)
76. A M Ali, E A C Emanuelsson, D A Patterson *Appl. Catal., B* **97** 168 (2010)
77. E Finocchio, G Busca, V Lorenzelli, R J Willey *J. Chem. Soc., Faraday Trans.* **90** 3347 (1994)
78. K Ramesh, L Chen, F Chen, Y Liu, Z Wang, Y-F Han *Catal. Today* **131** 477 (2008)
79. H Over, Y D Kim, A P Seitsonen, S Wendt, E Lundgren, M Schmid, P Varga, A Morgante, G Ertl *Science* **287** 1474 (2000)
80. E Finocchio, G Busca, V Lorenzelli, V S Escribano *J. Chem. Soc., Faraday Trans.* **92** 1587 (1996)
81. W-P Han, M Ai *J. Catal.* **78** 281 (1982)
82. B M Reddy, in *Metal Oxides: Chemistry and Applications* (Ed. J L G Fierro) (Boca Raton, FL: CRC Press, Taylor and Francis, 2006) p. 2115
83. E V Starokon, MV Parfenov, L V Pirutko, S I Abornev, G I Panov *J. Phys. Chem. C* **115** 2155 (2011)
84. A Bielański, M Najbar *J. Catal.* **25** 398 (1972)
85. C R A Catlow, R A Jackson, J M Thoma *J. Phys. Chem.* **94** 7889 (1990)
86. Y Barbaux, A Elarmani, J P Bonelle. *Catal. Today* **1** 147 (1987)
87. G I Panov, K A Dubkov, E V Starokon *Catal. Today* **117** 148 (2006)
88. H-F Liu, R-S Liu, K Y Liew, R E Johnson, J H Lunsford *J. Am. Chem. Soc.* **106** 4117 (1984)
89. N Yamazoe, K Shimanoe *Sens. Actuators, B* **128** 566 (2008)
90. M Batzill, U Diebold *Prog. Surf. Sci.* **79** 47 (2005)
91. J Maier, W J Göpel *Solid State Chem.* **72** 293 (1988)
92. T Sahm, A Gurlo, N Bársan, U Weimar *Sens. Actuators, B* **118** 78 (2006)
93. A Gurlo *ChemPhysChem* **7** 2041 (2006)
94. G Korotcenkov *Sens. Actuators, B* **107** 209 (2005)
95. E K Kazenas, Yu V Tsvetkov *Isparenie Oksidov* (Evaporation of Oxides) (Moscow: Nauka, 1997)
96. M N Rumyantseva, E A Makeeva, S M Badalyan, A A Zhukova, A M Gaskov *Thin Solid Films* **518** 1283 (2009)
97. S Aksel, D Eder *J. Mater. Chem.* **20** 9149 (2010)
98. V V Kovalenko, A A Zhukova, M N Rumyantseva, A M Gaskov, V V Yushschenko, I I Ivanova, T Pagnier *Sens. Actuators, B* **126** 52 (2007)
99. W C Conner, J L Falconer *Chem. Rev.* **95** 759 (1995)
100. D D Frolov, Y N Kotovshchikov, I V Morozov, A I Boltalin, A A Fedorova, A V Marikutsa, M N Rumyantseva, A M Gaskov, E M Sadovskaya, A M Abakumov *J. Solid State Chem.* **186** 1 (2012)
101. *NIST Chemistry WebBook, NIST Standard Reference Database* No 69 (Eds P J Linstrom, W G Mallard) (Gaithersburg, MD: National Institute of Standards and Technology, 1983; http://webbook.nist.gov (retrieved, 2012)
102. N Sergent, P Gélin, L Périer-Camby, H Praliaud, G Thomas *J. Therm. Anal. Calorim.* **72** 1117 (2003)
103. A Davydov *Molecular Spectroscopy of Oxide Catalyst Surfaces* (Chichester: Wiley, 2003)
104. A Cabot, J Arbiol, J R Morante, U Weimar, N Bársan, W Göpel *Sens. Actuators, B* **70** 87 (2000)
105. A V Marikutsa, M N Rumyantseva, L V Yashina, A M Gaskov *J. Solid State Chem.* **183** 2389 (2010)
106. J T Hirvi, T-J J Kinnunen, M Suvanto, T A Pakkanen, J K Nurskov *J. Chem. Phys.* **133** 084704 (2010)

107. S Wang, Y Wang, J Jiang, R Liu, M Li, Y Wang, Y Su, B Zhu, S Zhang, W Huang, S Wu *Catal. Commun.* **10** 640 (2009)
108. I X Green, W Tang, M Neurock, J T Yates Jr *Science* **333** 736 (2011)
109. O V Krylov *Getrogennyi Kataliz* (Heterogeneous Catalysis) (Moscow: Akademkniga, 2004)
110. V V Yushchenko *Zh. Fiz. Khim.* **71** 628 (1997) [b]
111. V A Burmistrov *Gidratirovannye Oksidy Elementov IV i V Grupp* (Hydrated Oxides of Groups IV and V Elements) (Moscow: Nauka, 1986)
112. M W Abee, D F Cox *Surf. Sci.* **520** 65 (2002)
113. S C York, M W Abee, D F Cox *Surf. Sci.* **437** 386 (1999)
114. C S Rout, M Hegde, C N R Rao *Nanotechnology* **18** 205504 (2007)
115. H Mortensen, L Diekhoner, A Baurichter, E Jensen, A C Luntz *J. Chem. Phys.* **113** 6882 (2000)
116. E Guglielminotti, F Boccuzzi *J. Chem. Soc., Faraday Trans.* **87** 337 (1991)
117. F Boccuzzi, E Guglielminotti *Sens. Actuators, B* **21** 27 (1994)
118. D A Hansgen, G Vlachos, J G Chen *Nature Chem.* **2** 484 (2010)
119. N Sergent, M Epifani, E Comini, G Faglia, T Pagnier *Sens. Actuators, B* **126** 1 (2007)
120. P G Harrison, E W Thornton *J. Chem. Soc., Faraday Trans. 1* **72** 2484 (1976)
121. N V Ravlenko, A I Tropil'skii, G I Golodets *Teor. Eksperim. Khim.* **21** 315 (1985) [c]
122. V V Krivetsky, D V Petukhov, A A Eliseev, A V Smirnov, M N Rumyantseva, A M Gaskov, in *Nanotechnological Basis for Advanced Sensors* Vol. 32 (Eds J P Reithmaier, P Paunovic, W Kulisch, C Popov, P Petkov) (Dordrecht: Springer, 2011)
123. T Jinkawa, G Sakai, J Tamaki, N Miura, N Yamazoe *J. Mol. Catal., A: Chem.* **155** 193 (2000)
124. H Idriss, E G Seebauer *J. Mol. Catal. A: Chem.* **152** 201 (2000)
125. Z Zhou, H Gao, R Liu, B Du *J. Mol. Struct. (THEOCHEM)* **545** 179 (2001)
126. M Šulka, M Pitoňák, P Neogrády, M Urban *Int. J. Quant. Chem.* **108** 2159 (2008)
127. N Sergent, M Epifani, E Comini, G Faglia, T Pagnier *Sens. Actuators, B* **126** 1 (2007)
128. J D Prades, A Cirera, J R Morante, J M Pruned, P Ordejón *Sens. Actuators, B* **126** 62 (2007)
129. E Leblanc, L Perier-Camby, G Thomas, G Giber, R M Primet, P Gelin *Sens. Actuators, B* **62** 67 (2000)
130. M Ivanovskaya, E Lutynskaya, P Bogdanov *Sens. Actuators, B* **48** 387 (1998)
131. A Chiorino, G Ghiotti, F Prinetto, M C Carotta, M Gallana, G Martinelli *Sens. Actuators, B* **59** 203 (1999)
132. H Jeon, M Jeon, M Kang, S Lee, Y Lee, Y Hong, B Choi *Mater. Lett.* **59** 1801 (2005)
133. V B Zaytsev, A A Zhukova, M N Rumyantseva, A A Dobrovolsky, L Calvo, A M Gaskov *J. Cryst. Growth* **312** 386 (2010)

[a] — *Russ. J. Anal. Chem. (Engl. Transl.)*
[b] — *Russ. J. Phys. Chem., Ser. A (Engl. Transl.)*
[c] — *Theor. Exp. Chem. (Engl. Transl.)*